

“Jamila’s” Necklace: Study and Reconstruction of a Complex Ornament Found in the Child Burial CG7

HALA ALARASHI

Introduction

During the excavations in 2018, in the frame of the *Household and Death Project*, a cist-type burial (CG7; Fig. 1a-d) was uncovered in Room CR36.1. It revealed the skeletal remains of a child (Loc. C1:46) along with an impressive number of beads (F.no. 100814) (Gebel *et al.* 2019) found around her neck and on the chest. The excavation was conducted carefully to document simultaneously the relation between the skeleton and the beads. The position, articulation and preservation of the bones were described elsewhere (Benz *et al.* 2020; see also Gresky this volume). Due to the uniqueness of this burial and its sophisticated ornament, an additional funding was granted by the German Research Foundation (BO 1599/16-1) to analyse, conserve, and reconstruct the necklace. Results of the investigation on this complex ornament and its hypothetical reconstruction are described in this chapter. For the results of the geochemical analyses of the raw materials the reader is referred to the contribution by Melissa Gerlitzki and Manfred Martin (this volume). The conservation of the necklace is described by Alice Costes and Andrea Fischer (this volume), the reconstruction of the grave by Hussein M. al-Sababha and his colleague (this volume).

The body of the child was found resting on the left side in a crouched position (Fig. 1d). This position, along with the post-depositional conditions in the grave and gravity, have altered the positions of the beads in the upper layers where they were quite scattered and with no clear organisation (Fig. 1e-f). Several concentrations and alignments emerged progressively, while digging towards the bottom of the grave (Fig. 1l-o). The probability that the beads were simply and randomly deposited on the upper parts of the body was excluded, as series of beads showed patterns of organisation. Thus,

several questions were formulated straightaway during the excavation:

1. Were these beads part of the same composition, and if so, what was the type of ornament in which they were integrated: a necklace, a plastron, a decorated garment?
2. How and of which materials were they made?
3. Were they made and assembled at Ba`ja or imported from elsewhere?
4. Were they used or manufactured for the occasion of interment?

To provide responses, the finds were analysed:

- as single entities in order to address the types, sizes, manufacture and use processes,
- as series, groups, or rows according to their location in the grave in order to understand the type of ornament they composed.

Observations and First Hypotheses

The complexity of the composition was recognised gradually during the excavation (Fig. 1d-o). Observations made in the field were essential to build a global understanding of the assemblage, such as the associations between the beads and the bones, their dynamics and densities among the excavated layers, and their arrangements. The following observations were made in the field:

- The right side of the skeleton was damaged with some bones of the upper layers having completely vanished. The beads associated to the right side of the neck and the ribs (Figs. 1e-f, 3a-c), which were the first to be excavated, were scattered around the upper body, showing no clear association or organisation. The density increased, and alignments of beads appeared down towards the left side of the skeleton, while continuing the excavation (Fig. 1n-o). The density decreased when the bones of the left



Fig. 1 (left page) The cist-type burial, the child, and the progress of the excavation of the associated ornamental items: *a-c* the burial sealed with different types and layers of sandstone slabs; *d* the skeletal remains of the child inside the opened burial; *e-f* the appearance of the ring around the neck area with scattered little concentrated groups of beads; *g* view of the ring in its vertical position; *h* increased density of the beads after the removal of the ring and the appearance of a black element below the cervical vertebra; *i* beads stuck to the perforation of the black element and appearance of an additional turquoise bead (note the fragmentation and the displacement of the mandible); *j* the *manubrium* and a spherical black bead on its upper left; *k* another spherical black bead appeared just after the removal of the *manubrium*, placed at its upper right; *l-o* increased density of the beads in alignments in the area between the left *clavicula* and the left mandible (removed). (Photos: *a-c,e,n,o*: M. Benz; *d,f,m*: H. Alarashi, Ba`ja N.P)

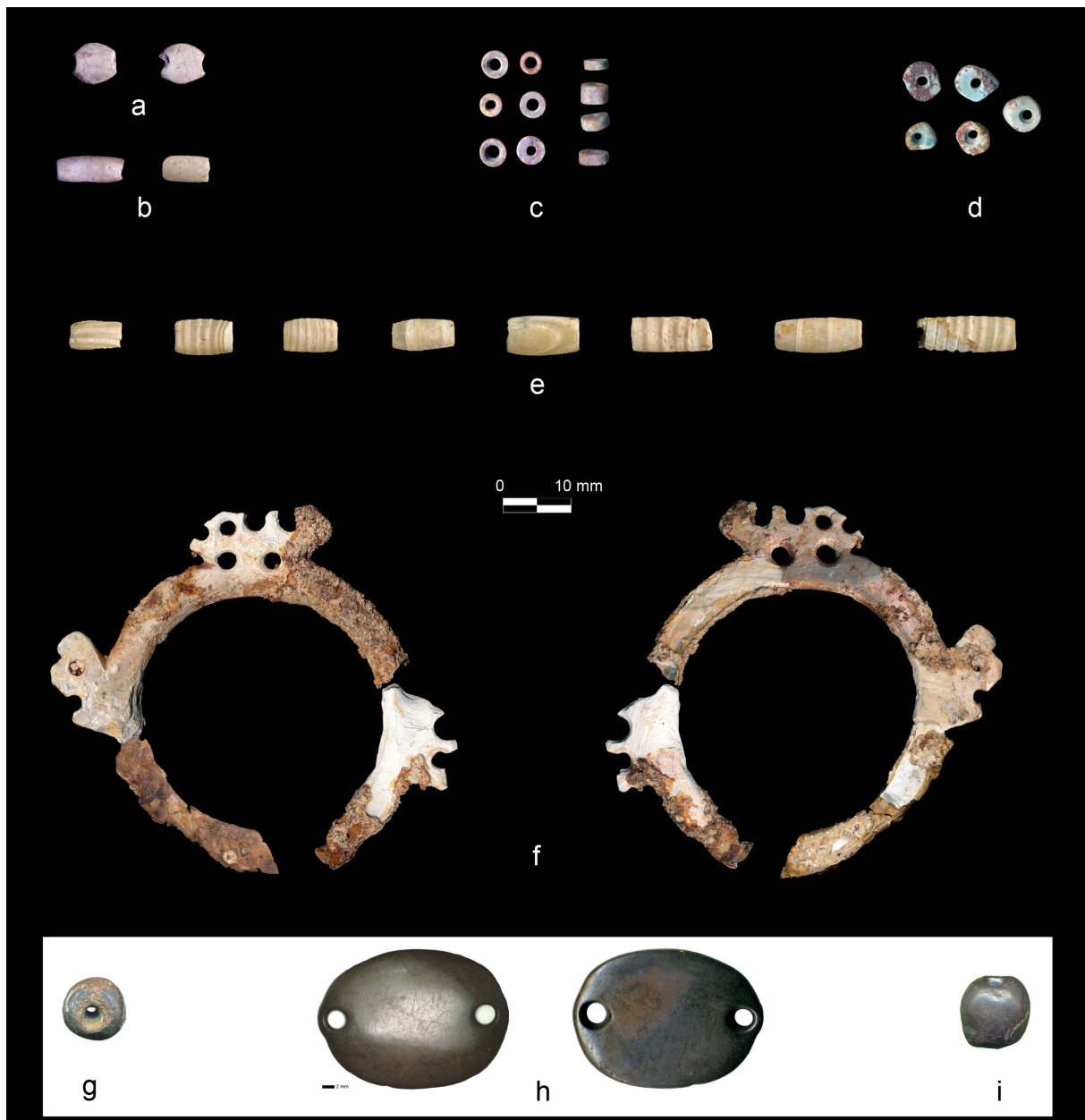


Fig. 2 Examples of beads representing: *a-e,g,i* the typological diversity and *f* the exceptionally large mother-of-pearl (MOP) ring and *h* a hematite double perforated object. (Photos: *a-e,g-h*: H. Alarashi, *f*: A. Costes, Ba`ja N.P.)

- side (*clavicula*, *scapula*), *i.e.*, the lowest layers of the skeleton, had been removed from the silty sand (Fig. 1e-i).
- Beads were neither found under the arms, on the lateral side of the torso nor on the back along the thoracis or the lumbar vertebrae. The elements were strictly distributed on the upper part of the chest and around the neck (Fig. 1e-o).
 - Most items were tiny discs (Fig. 2c) followed by tubular white shell (Fig. 2e) and red limestone beads (Fig. 2b). In addition, an impressive mother-of-pearl ring (Fig. 2f) with many perforations and a large double perforated black pendant (“buckle”) (Fig. 2h) were found in a central position regarding the dispersal area of the ornament, very close to the cervical vertebra and behind it respectively. Some beads still stuck to the perforations of these two unique pieces (Fig. 1g,i). Other rare elements are turquoise beads (n=5) (Fig. 2d), flat sub-oval beads (n=7) (Fig. 2a), and two spherical black beads (Fig. 2g,i).
 - Disc beads were distributed all over the area of the neck and chest. Some isolated beads were also present in unexpected places, such as behind the skull near the occipital bones, or the facial bones. It seems that they have been rolled down from their initial position after the decomposition of the string, or moved by other taphonomic processes and disturbances by bioturbation.
 - The mother-of-pearl ring was found in a vertical position on its edge (Fig. 1g). Its upmost edge was quite damaged (Fig. 3a-b), and it appeared simultaneously when the first beads started to appear (Fig. 4a). There were only a few beads uncovered at the level of its upper parts, but they started to increase near its bottom (Figs. 3d-e, 4a-c). It was necessary to remove all the sediment covering the ring (Fig. 3d-h) and remove it to notice that it was laying between the chest and the mandible.
 - The skull was damaged and fragmented (Figs. 1e, 3a,c, 4a-b), with the right side of the mandible being decayed and the teeth scattered. A molar was found very close to the mother-of-pearl ring (Fig. 3b).
 - The “buckle” was discovered under the left side of the cervical vertebra (Fig. 1h-i) and next to the ring. Both objects seem to have moved from their initial position, due to gravity as the corpse was resting on its left side.
 - One compact spherical bead was found between the neck and the *manubrium* (slightly to the east of the *manubrium*) (Fig. 1j), while another similar one was found at a lower position close to the left side of this bone (on the right side in the photo) (Fig. 1k).
 - Groups of tens of beads were found tightly aligned in a chain-like organisation, and some remained stuck in this position (Fig. 1h-o). The alignments occurred at several depths and in distinct parts of the distribution area.
 - Tubular white beads were more concentrated in the area corresponding to the left *clavicula* and the left side of the cervical spine (Figs. 1m-o, 4c). They tend to be aligned in groups of two, preceded and followed by several series of red disc beads.
 - Rare objects such as the turquoise beads were found in different parts of the ornament area, some within concentrations or groups of aligned beads, yet rather on the front side of the neck or the chest (Fig. 1i,o).
- The above-mentioned observations made during the excavation led us to formulate several hypotheses discussed in detail in the results’ section:
- The beads, the mother-of-pearl ring, and the “buckle” were part of a composition displayed around the neck and on the chest of the child.
 - The beads were not sewn or fixed individually to a garment or a cloth, but were threaded on strings to comprise several rows, as suggested by the connection of beads with the ring and the “buckle”, and by the alignments of beads distributed in several places. This was also confirmed by the use-wear analyses, described in detail in the results section, as several beads show frictional traces diagnostic of chain-like alignments.
 - The mother-of-pearl ring was found on the left mandible (Fig. 3d-h), a position most likely due to gravity occurring when the child was laid down in the grave. Additionally, it should be stressed that the skull was strongly damaged and fragmented. The mandible was separated from the skull and displaced. Due to the decaying flesh and ligaments, the ring slipped into the mandible and was uncovered resting on the left part of it.
 - The mother-of-pearl ring played a key-role in structuring the ornament because of its central position within the area of concentration/ dispersal of the beads, but



Fig. 3 The excavation of the ornament with a focus on the MOP ring: *a* the upmost part of the ring; *b* with its edge very damaged; *c* the location of the ring in the area of the neck, between the fragmented skull and the chest; *d-e* the ring with the first aligned disc bead (note the poorly preserved, broken right mandible just to its right); *f-g* a vertical view of the ring showing shaped outgrowths around its major diameter; *h* the lowest edge of the ring reached, with one large tubular bead near one of its perforations; *i* concentrations of beads appearing after the removal of the ring. (Photos: *a-c*: M. Benz; *d-i*: H. Alarashi, Ba'ja N.P.)

also because of its uniqueness, large size, decorative features, and the number of its perforations distributed all around its circumference. It is therefore reasonable to think that it was intended to be displayed on the chest, or even on the tummy, as these positions allow better spreading of the rows of beads, a better display of the beads' diversity, and better visibility of the ring itself.

- The orientation of the ring was determinant for the estimation of the number of rows and for understanding the way the ornament was planned to be exhibited on the body.
- The position of the body in the grave placed on the left side explains the density of concentration of beads on the left side, as part of those from the right side may have fallen on them after the decomposition of the organic tissues (strings and body of the child). An important number of beads has been displaced and mixed with others.
- The turquoise and hematite beads were placed in special frontal places in order to enhance their visibility and to accomplish specific functionalities.

Methods

Excavation and Documentation

All the elements of the ornament were precisely documented in the field in order to understand the original composition of different elements. When the beads started to appear, they were given proper numbers, and their position was drawn and documented individually using a cartesian coordination system (x, y, z). The elements were sketched layer by layer during the excavation (Fig. 4a-c). This method was applicable as long as the beads appeared in few numbers, scattered, and isolated. The discovery was, however, out of our expectations; as we continued the excavation, the beads appeared in significantly increased numbers, found in concentrations and organised small groups, which required a readjustment of the method of documentation due to time constraints. Therefore, the beads were described, sketched (Fig. 4a-c) and photographed in groups, while respecting as much as possible their positions and alignments by introducing, very gently and carefully small pins (Fig. 1f-g,n-o). Otherwise, it would have been impossible to preserve

these organisations due to the very loose sand, in which the child was interred.

It was very important to dig as fast as possible in order to preserve the skeletal remains and the finds. The excavation of the burial lasted one week during which the work became a challenge of patience and physical endurance because of:

1. the far access to the area of the beads laying at the bottom, at more than 60cm deep from the upper level of the grave (Fig. 1c);
2. the impossibility to excavate from the eastern, northern, or southern sides of the burial because of the surrounding walls. The only access was from the west, laying on the body (Fig. 5); stretching the arms, with one hand supporting the weight of the body, while the other excavating;
3. the instability of the beads laying on sandy, very loose sediments.

After the documentation, the beads were taken off and packed in bags and boxes. A specific labelling system was followed. A field number (F.no. 100814) was assigned to the whole ornamental composition. Proper numbers were assigned to the first 169 beads (from F.nos. 100814.0 to 100814.168), whereas letters were given to the groups of (Fig. 4b-c, D7-D10) elements that started to appear later (from F.nos. 100814.A to 100814.AA). Within these groups, series of successive beads were distinguished using roman letters (*e.g.*, F.no. 100814.M.IX).

The ornament has suffered post-depositional alterations and many beads had calcifications. Several were agglomerated, preventing their examination or even counting. Therefore, with the help of Alice Costes (*cf.* below), the elements were sorted into two groups:

- the group of Stuttgart (**GS**) that contained 888 items (35%) and needed cleaning, consolidation, and/ or restoration. They were handled by Alice Costes and her supervisor Andrea Fischer from the State Academy of Art and Design Stuttgart (Germany);
- the group of Nice (**GN**), consisting of 1697 relatively well-preserved items (65%) on which it was possible to carry out several macro- and microscopic diagnoses and analyses. The study of this group was carried out at the CEPAM laboratory (CNRS-UMR 7264), at the University Nice Côte d'Azur (France).

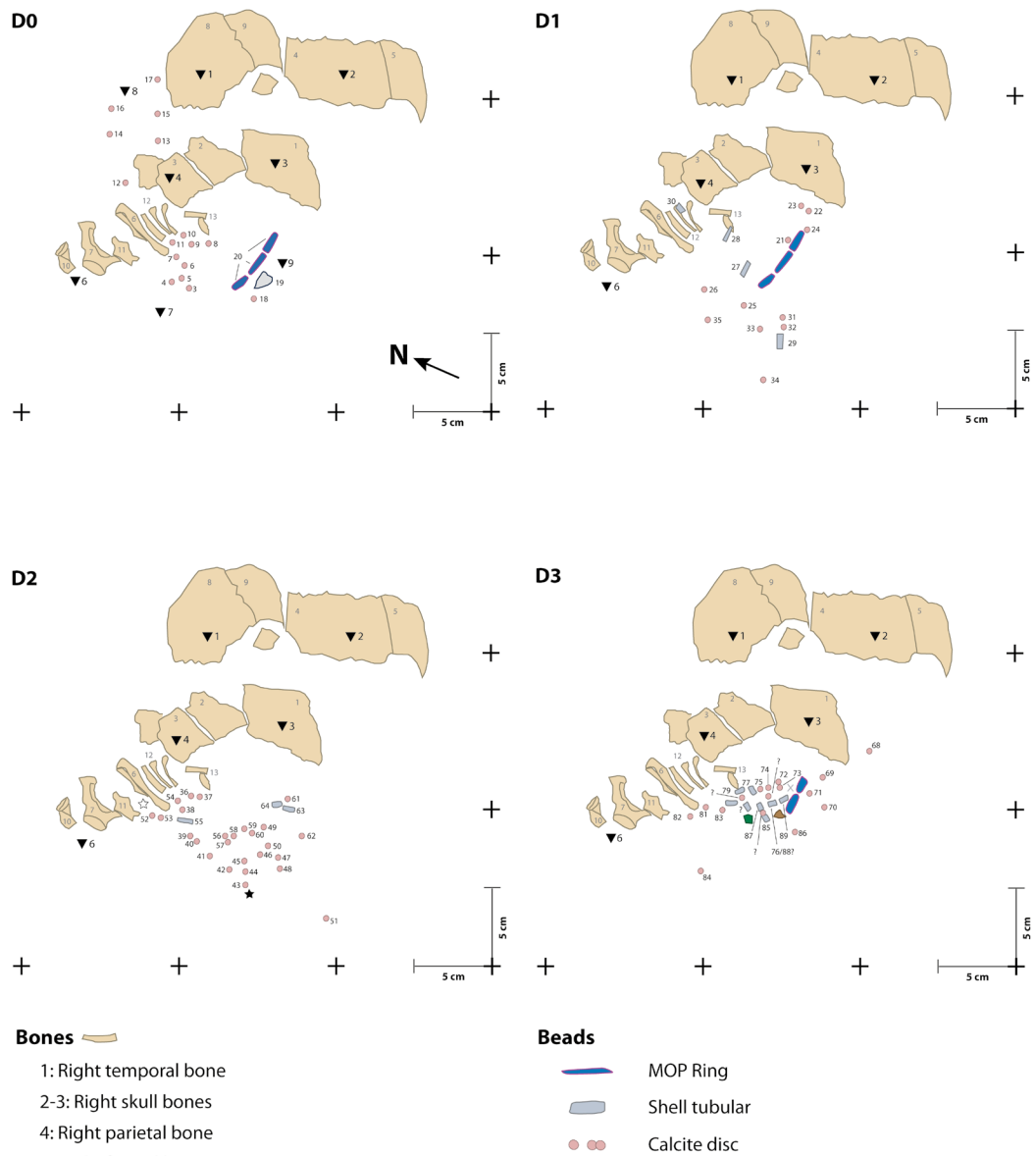


Fig. 4a Four uppermost layers of beads in Burial CG7. (Sketches: H. Alarashi, digitalisation: J. Rolke, Ba'ja N.P.)

Identification of Raw Materials

Different elements of the ornament were made of minerals and marine shells. This first classification was based on the visual aspects (colour, textures) of the surfaces, and on the inner matrix exhibited when some beads were broken. Chemical and structural analyses were performed to refine the identification of items within each group (Table 1).

Typology and Morphometry

The diversity of morphological types was determined based on an established typological classification (Alarashi 2014). All the elements were 2D scanned using *Epson Perfection 4490 PHOTO* scanner. Only those of GN (*cf. supra*) were measured and morphometrically analysed. Basic measurements were made manually using an electronic calibre, with values filled

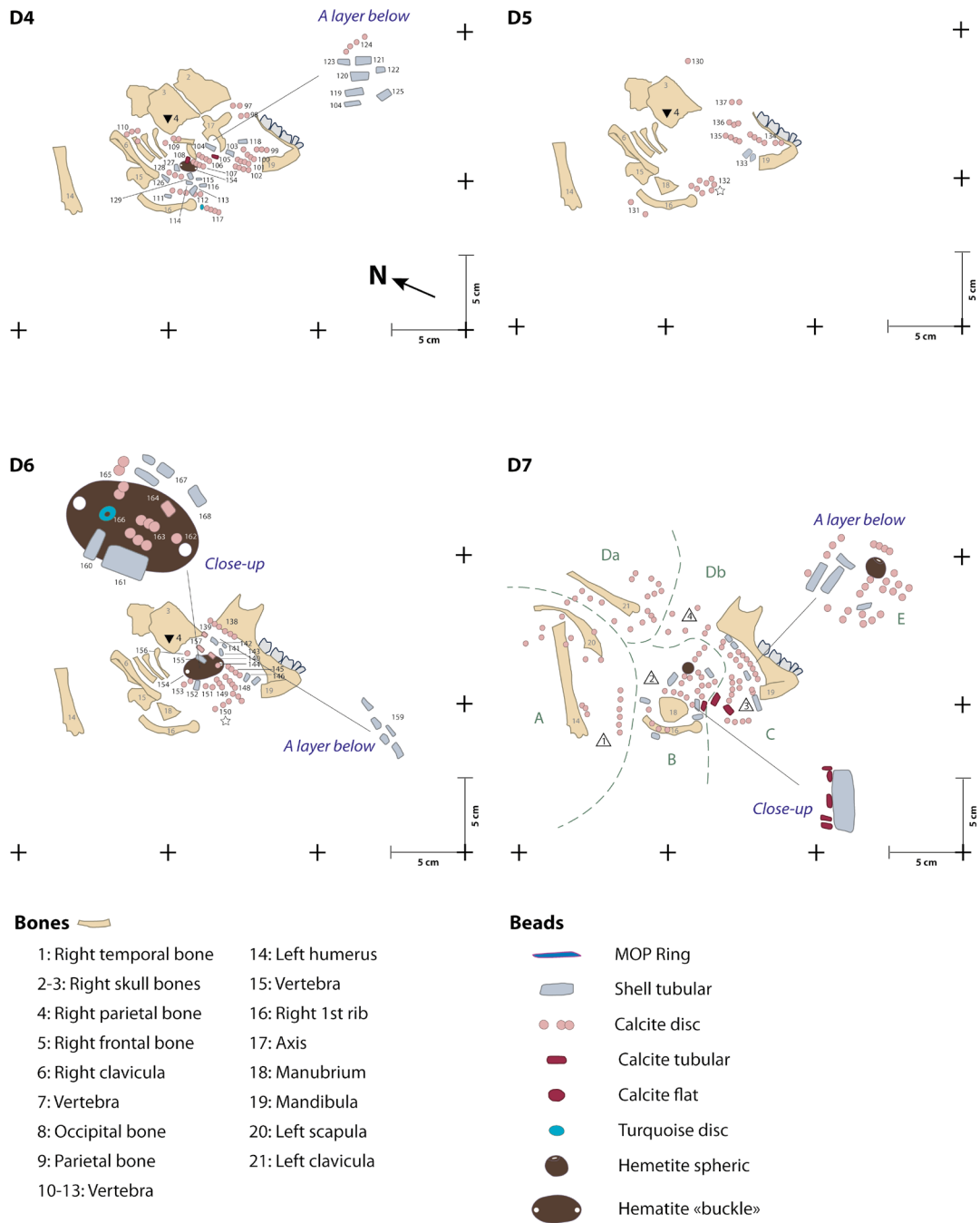


Fig. 4b Four middle layers of beads in Burial CG7. (Sketches: H. Alarashi, digitalisation: J. Rolke, Ba`ja N.P.)

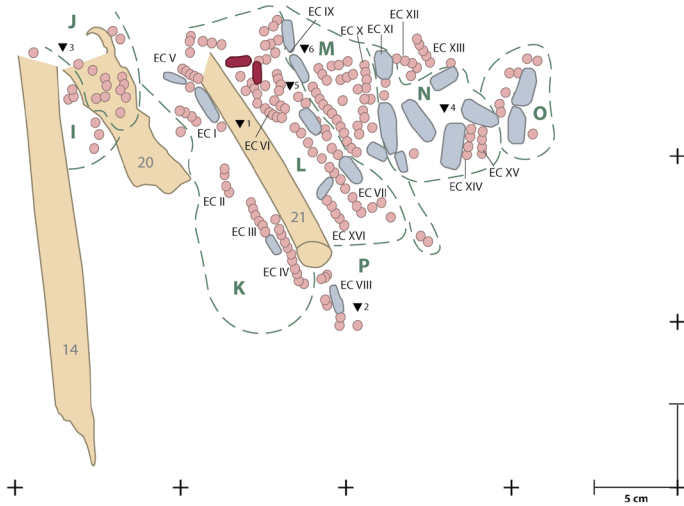
automatically on an excel sheet. For the disc beads the diameter, the diameter of perforation, the degree of roundness, and circularities were calculated through *Shape Recognition System* by applying informatic scripts programmed by the author using a free online image treatment software (*ImageJ Fuji*). The fragile mother-of-pearl ring was measured on its scanned image. The tubular white beads have natural motives in the shape of parallel strips. These were described according to the main major axis of the

bead (perpendicular, parallel, and oblique), in order to examine any correlation between these patterns and the emplacement of the bead within the ornament.

Macro- and Microscopic Observations

Due to its poor state of preservation and fragility, the mother-of-pearl ring was examined using a digital portable microscope (*Dino-Lite Edge 5m, 20X – 200X*) in order to avoid any manipulation

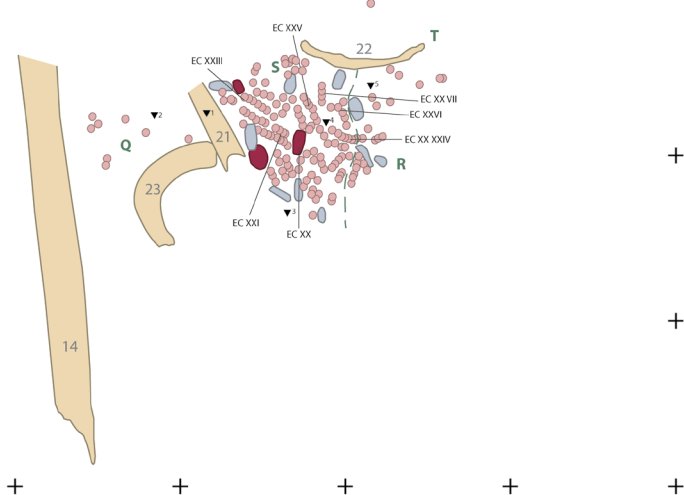
D8



Bones

- 14: Left humerus
- 20: Left scapula
- 21: Left clavicle
- 22: Skull left fragment
- 23: Left rib

D9



Beads

- Shell tubular
- Calcite disc
- Calcite tubular
- Calcite flat
- Turquoise disc

D10

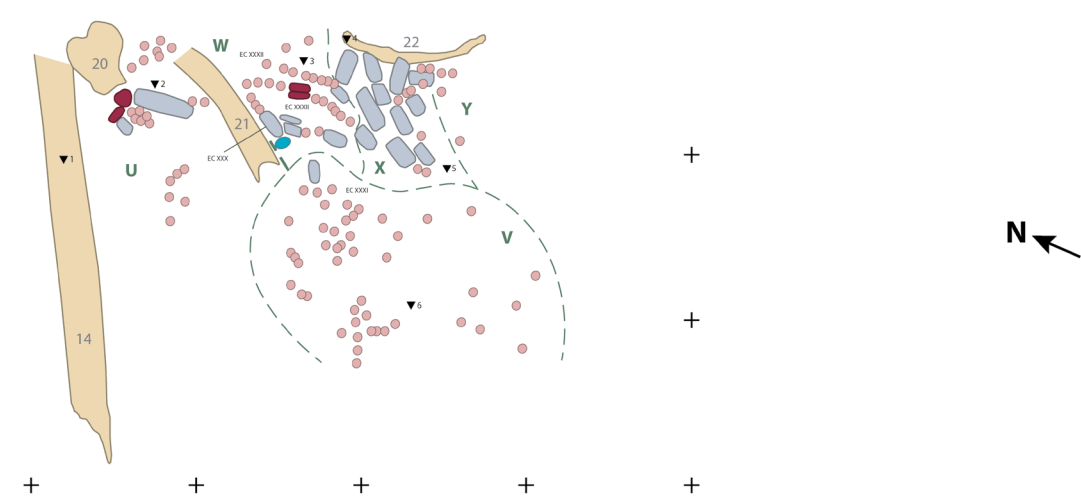


Fig. 4c Three lowermost layers of beads in Burial CG7. (Sketches: H. Alarashi, M. Benz, digitalisation: J. Rolke, Ba'ja N.P.)



Fig. 5 Challenging excavation due to severe space constraints. Marion Benz (upper photo), with Hala Alarashi handling tools (lower photo). (Photos: H.G.K. Gebel, Ba`ja N.P.)

as much as possible. The study took place in the laboratory of Stuttgart before the restoration process. The GN objects were all examined by the naked eye. The types and sections of perforations were described. Microscopic traces related to the manufacturing and use-wear processes were recorded on a selection of objects representing

the diversity of raw materials and morphological types. First observations were made in the excavation base camp in 2018, using a binocular stereoscope (*Euromex SteroBlue 0.7X–45X*). A microscope (*Leica Z16 APO 0.7X–90X*) equipped with a digital camera was then employed at the CEPAM laboratory in Nice.

Table 1 Methods of analyses, laboratories, and results. *A pilot study applied on shell beads from another children burial (CG9, Loc. CR28.2:122a-b/ 123a-b), yet identical to those found in Grave CG7, Loc. C1:46 of Room CR36.1.

Method	Laboratory/ University
X-Ray fluorescence	Landesamt für Geologie, Rohstoffe und Bergbau (LGRB) Regierungspräsidium Freiburg (M. Gerlitzki, M. Martin)
X-Ray diffraction	CEMEF - Centre de Mise en Forme des Matériaux, University Sophia Antipolis (G. Monge)
ATR-FTIR	Labor für Konservierungswissenschaften und Archäometrie, Stuttgart (J. Schultz)
FTIR	Institute for Material Science (CSIC–University of Seville), Sevilla (C. Odriozola Lloret, J. Ángel Garrido Cordero, M. Ángel Avilés)
C/ O - Isotopes	Institut de Ciència i Tecnologia Ambientals (ICTA-UAB), Barcelona (A. Carlo Colonese)
ZooMS*	Department of Life Sciences and Systems Biology, University of Turin (B. Demarchi)

Reconstruction of the Ornament

The reconstruction method adapted is based on a “DNA sequencing” philosophy, in the sense that some of the results were obtained from observations of short sequences or portions of beads discovered *in situ*.

The Mother-of-Pearl Ring

The mother-of-pearl ring was highly damaged when it was discovered (Fig. 3). The nacre was disintegrated into fragile layers, and a small portion had completely vanished. Yet, its careful excavation allowed us to collect two complete fragments: a half and a quarter of the ring. The other quarter, the first excavated and the most damaged, was collected into several pieces that were re-fitted together by the conservators, thanks to the documentation made in the field and by studying the shape of the ring. The whole ring was cleaned and consolidated by Alice Costes. Because of several missing parts, the reconstruction of the ring proposed here (*cf.* results) is hypothetical. It relies on the shape of the preserved fragments, on measurements, and on comparisons with a similar ring found at the site in the collective Burial DG1, in Area D in 2000 (Fig. 17, F.no. 30408; Gebel and Hermansen 2001).

Measurements, Weight, and Volume: Estimations

The length (*i.e.*, the thickness of the disc-shaped objects) of all the beads from GN (65% of the total) was measured in order to estimate the total length when aligned tightly one after the other. The results were used to estimate the length of the non-measured beads (GS), in order to estimate the length of all the beads when aligned in a chain-like arrangement. This was necessary to examine the adequacy of the volume of the ornament when exhibited on an 8-10-year-old child’s body.

The estimated length (minimum, average, and maximum) of the ornament as a single row of beads was divided by the number (n) of perforations in the ring, in order to further estimate the number of rows that structured the ornament.

The number of beads by type was divided by the number of rows according to the minimum, maximum, and main lengths of strings. The arrangement of beads per type within each row was based on the results of these divisions, and on the alignments documented *in situ* in the field. The total number of beads (all types) and their arrangement within each row was then established.

Additionally, samples of beads per type were weighed. The results were used to estimate the total weight of the elements that make up the ornament, excluding the strings used in its composition, for which we have no evidence regarding their nature(s) or treatments (*e.g.*, with added ochre). The weight of the mother-of-pearl ring was estimated based on its measurements.

The distribution of rows followed the principal of symmetry and equilibrium, which ensures the optimal position of the ornament when exhibited. The volume and spread of the ornament on the body was estimated considering standard measurements of the neck, shoulders, arms, and torso of children of both sexes between the ages of seven and nine according to the AFNOR: French Standardization Association.

Results

The results will first be presented at the level of the single or group of elements, then discussing the whole composition after all the elements had been assembled together.

Raw Materials

Minerals are predominantly used, followed by marine shells. To these two “classical” categories of raw materials, a third, very rare, is represented by two beads made from fossil resin.

Minerals

The amounts of the chemical elements composing eight samples of beads were measured by XRF. They confirm the preliminary visual identification made by the author: calcite, turquoise, and hematite (Fig. 6, see also Gerlitzki and Martin this volume).

Thin sections of three samples and XRF-analyses of reddish disc beads identified them as calcite. The percentage of the chemical elements indicate over 90% of CaO, which can be interpreted as a highly pure variety of calcite. The reddish nuances are related to the presence of iron (Fig. 7).

X-Ray diffractometry measurement (Fig. 8) applied on the powder of a small fragment of bead has confirmed the identification of the calcite made by the XRF.

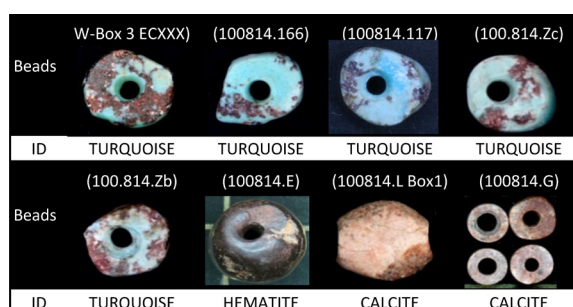


Fig. 6 The beads analysed by XRF and the identification of their raw materials. (Photo: H. Alarashi, Ba`ja N.P.)

This calcite, which has also been used for tubular and flat beads (Fig. 2a-b), is soft (under 4 on Mohs hardness scale) with compact, relatively homogenous grains that seem to allow the material to transform smoothly without much risk of fracture.

The five green disc beads (Fig. 6) were all identified as turquoise, which is a relatively hard mineral (5-5.5 on Mohs scale).

XRF measurements show different percentages of the chemical elements, yet with relatively high amounts of those typical of turquoise (Gerlitzki and Martin this volume: Table 1). Those found in the burial all have a dark, wine-coloured gang-like full of translucent crystals, possibly quartz. Turquoise with similar inclusions are recorded from another burial at Ba`ja (Benz *et al.* 2019). The turquoise-green colour strongly contrasts with these inclusions.

Items made from hematite have a high concentration of iron. Only three were found in the burial, but they are relatively large (Fig. 2g-i). This mineral is hard (5.5-6.5 on Mohs scale) and is characterised by its metallic lustre and brown reddish colour due to its iron oxide composition.

Shells

The ring was made from a large specimen of a *Pinctada margaritifera*, a common Red Sea bivalve shell frequently exploited in the southern Levant (Bar-Yosef Mayer 2005; Abu Laban 2014; Spatz *et al.* 2014), especially at Ba`ja (Alarashi a this volume).

XRF measurements made on one tubular white bead (found in another context), which is identical to those of Burial CG7, indicate an aragonite

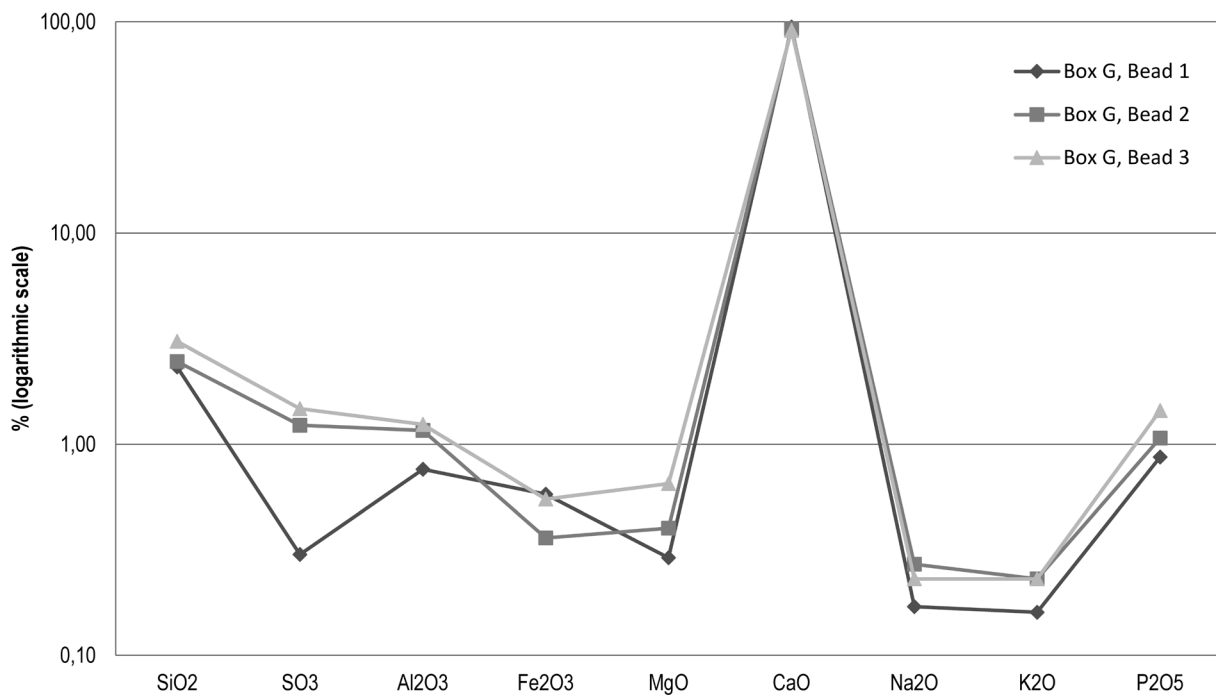


Fig. 7 Percentage of the chemical elements composing the reddish disc beads based on XRF measurements of thin sections by M. Gerlitzki and M. Martin. (Graph: M. Benz, Ba'ja N.P.)

and carbonate composition identical to those of the marine shells. These beads were previously identified as being made of fossil *Tridacna* sp.¹ (D. Reese, personal communication). Analyses of carbon and oxygen isotopes made on identical beads from another burial (CG9), were not conclusive enough to determine whether these shells originated from the Mediterranean or the Red Sea, as the values from these two seas are quite similar. They confirm however a maritime origin and exclude any freshwater source (A. Colonese, UAB). Proteomic analyses (*ZooMs* by B. Demarchi, Univ. of Turino, see Table 1) applied on these samples confirmed that these beads were made from marine shells, precisely from *Tridacna* valves (Alarashi a this volume).

Four specimens of a very small *Conus* sp. shell were determined, along with a unique example of a *Dentalium* shell (Table 2). The gastropod and the scaphopod shells were sliced, those of *Conus* being tiny and short.

Resin

Two beads were identified as a fossil resin (analysis by J. Schultz, State Academy of Fine

Arts Stuttgart). They represent an exceptional category, never recorded for such an ancient period; they are the oldest discovered archaeologically so far (Fig. 9).

The result was confirmed through analyses performed in Sevilla (Spain). The set of recorded spectral features in the analysed samples are compatible with the spectral features recorded for amber from Lebanon (Kaur *et al.* 2012; Nohra *et al.* 2013). These beads were poorly preserved. Even though the grave filling was sieved with a 0.5mm sieve, it cannot be excluded that other tiny pieces of fossil resin beads have disappeared or were unobserved during the excavation as the sediments were similar in colour (especially where ochre powder or spots occurred).

Typological Diversity, Techniques, and Use-Wear Marks

The objects correspond to three typological groups (Fig. 2, Table 2): the beads (centred perforation), the double perforated pendants (bilateral perforations) and the rings (large perforation).

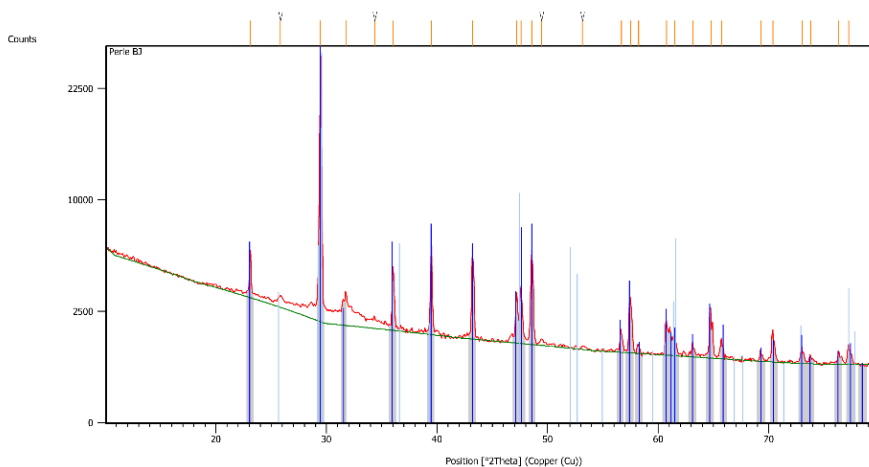
Each type is detailed separately, along with brief descriptions of the technical and use-wear traces when they were observed. It should be stressed that optimal cleaning

¹ For the sake of easy readability, in the following text we use the short form *Tridacna*, meaning *Tridacna* sp.

Measurement Conditions: (Bookmark 1)

Measurement Date / Time 21/05/2019 15:41:54
 Operator manip
 Raw Data Origin XRD measurement (*.XRDML)
 Scan Axis Gonio
 Start Position [°2Th.] 10,0814
 End Position [°2Th.] 79,9174
 Step Size [°2 Th.] 0,0790
 Scan Step Time [s] 141,2700
 Scan Type Continuous
 PSD Mode Scanning
 PSD Length [°2Th.] 3,35
 Offset [°2Th] 0,0000
 Divergence Slit Type Fixed
 Divergence Slit Size [°] 0,2500
 Specimen Length [mm] 10,00
 Anode Material Cu
 K-Alpha1 [Å] 1,54060
 K-Alpha2 [Å] 1,54443
 K-Beta [Å] 1,39225
 K-A2 / K-A1 Ratio 0,50000
 Generator Settings 30 mA, 45kV
 Diffractometer Type 0000000000004271
 Diffractometer Number 0
 Goniometer Radius [mm] 240,00

Visible	Ref. Code	Score	Chemical Formula	Compound Name	Mineral Name
*	01-072-1652	76	CaCO ₃	Calcium Carbonate	Calcite



Name and formula

Reference code: 01-072-1652
 Mineral name: Calcite
 Compound name: Calcium Carbonate
 ICSD name: Calcium Carbonate
 Empirical formula: CCaO₃
 Chemical formula: CaCO₃

Crystallographic parameters

Crystal system: Rhombohedral
 Space group: R-3c
 Space group number: 167

Fig. 8 XRD graph and information corresponding to the analysis of one disc bead fragment (powder) indicating the calcite mineral. (Measurement and Graph: G. Monge, CEMEF)

Table 2 Diversity of materials by functional types discovered in CG7, Loc. C1:46. Tub: tubular, Sph: spherical, DP: double perforated, Foss. resin: fossilised resin. *To this should be added 30 (?) broken fragments of disc beads.

Materials	Functional Types						Total
	Disc bead	Tub. bead	Flat bead	Sph. bead	DP pendant	Flat ring	
Minerals	Calcite	2264*	66	7	0	0	2337
	Turquoise	5	0	0	0	0	5
	Hematite	0	0	0	2	1	3
Marine shells	<i>Pinctada</i> sp.	0	0	0	0	0	1
	<i>Tridacna</i> sp.	0	232	0	0	0	232
	Dentalium	0	1	0	0	0	1
	<i>Conus</i> sp.	4	0	0	0	0	4
Foss. resin	Foss. resin	0	2	0	0	0	2
Total		2273	301	7	2	1	2585

(using water or ultrasound machine) was not carried out for the beads from GN in order to avoid excessive damage. Indeed, most of them are carbonate-based (calcite and shells) soft materials with altered, crackled surfaces. Similar alterations were even observed for harder materials (some turquoise [Fig. 10f] and hematite beads).

The manufacture of the stone and shell beads was carried out through a general transformation scheme composed of three stages: shaping, drilling, and finishing. Depending on the nature of the raw material and on the type of the bead, the techniques applied within each of these stages can vary. While macro- and microscopic traces were regularly observed for the drilling and finishing stages, those related to the shaping

were completely erased. Based on the study of shell and stone preforms of beads found in other contexts at the site, it seems that the shaping stage was mostly affected by abrasion, although the application of sawing for carbonate-based materials, or percussion for turquoise or hematite, cannot be excluded. The perforations were systematically made from both sides, regardless of the type of ornament element and the raw material. However the finishing stage that implies the regulation of the shapes was not systematic and appears conditioned by the type or the raw material.

As for the general state of use of the objects, macro- and microscopic observations revealed an intensive use of those recorded in few numbers, such as the turquoise and the hematite beads. Use-wear traces on the calcite and shell beads detected microscopically at low magnifications, were rather superficial and hardly developed.

Disc Beads

The bulk of the objects corresponds to the typological family of disc beads (Fig. 10). The most common type are regular small circular discs with sub-rectangular profile, made from reddish orange calcite (Fig. 10a-c). Beads with irregular sub-oval to polygonal shapes, made from turquoise (Fig. 10f-i) were also considered as discs, along with those identified as *Conus* shells circular slices (Fig. 10d-e). The raw materials used for this typological family offer contrasting colours: red, blue turquoise, and white. Yet, only the first two can have a visual effect as the *Conus* slices are rare and small.



Fig. 9 Two resin-based beads: a complete oval bead, b detail of the resin structure, c fragment showing the inner side of the bead and the resin in a cross section. (Photos: C. Odriozola Lloret)



Fig. 10 Typological diversity of the disc beads and technical and use-wear traces detected on the turquoise beads: a-c calcite circular disc beads, c last three examples to the right show variation in the degree of circularity due to the finishing process by batch abrasion, d-e *Conus* disc beads, f-k turquoise beads, j detail of picture h left, k detail of picture i left. (Photos: H. Alarashi, Ba'ja N.P.)

Calcite disc beads were manufactured according to the general method mentioned above (shaping, drilling, and polishing). The perforation was made from both sides, as attested by the bi-conical sections. However, the cylindrical section is also quite recurrent and can be explained by an intentional enlargement of the initial hole. This was not systematic and might have taken place during the threading process of the beads in order to enable the stringing. On the other hand, the shape of the discs is regular, with a high level of circularity and standardised size (*cf.* morphometric data below). These features are typical of batch or *en masse* (Francis 1989; Wright *et al.* 2008) processing during the finishing stage, such as the serial abrasion of the profile of strung beads in a back-and-forth movement parallel to the axis of the string.

Batch processing can also produce fractures on the profiles. Thus, sometimes unusual shapes can occur, as those observed on some calcite discs (Fig. 10c, the last three from the left).

The irregular shapes of the turquoise beads (Figs. 2d, 6, 10f-i) is observed for all the specimens found at the site, and not only in the child's burial (Benz *et al.* 2019, this volume; Gebel *et al.* 2020). Although their shaping and perforation were successful, it is possible that these irregularities were the results of constraints related to the quality of turquoise, and the presence of quartz-like reddish inclusions which might have significantly hardened the transformation of the material. Finally, the shiny polish of the surfaces, the strong rounding of the edges, and the erasing of the technical traces suggest that the turquoise beads were used intensively, and/ or for a long period. The homogeneity of the use-wear traces on the surface and inside the perforation indicates a free suspension, *e.g.*, aligned on the same string with other beads.

The *Conus* discs (Fig. 10d-e) are slices corresponding to the largest diameter of the shell whorl, with the missing apex allowing the perforation. The poor preservation didn't allow the identification of technical or use-wear traces. However the observation of well-preserved *Conus* discs from other contexts on the site indicate that the apex is usually eliminated by abrasion and the whorl is cut by sawing (Alarashi a this volume).

Tubular Beads

With a total of 298 specimens, tubular beads represent the second most important typological family of the assemblage. Two types were roughly distinguished between cylindrical (Figs. 11f-g, 14e) and "barrel"-shaped (Fig. 11a-e). For many beads the difference is subtle and depends on the side of the profile we observe. For both types, the section is sub-circular or oval. Most of the beads of this family are made from bivalve shells, namely *Tridacna* (Table 2, Fig. 11), while the other group is shaped from the same reddish calcite material used for the disc beads (Fig. 14d-f).

The bivalve fragments were transformed into tubular beads considering the natural alternated mat/ translucent growth lines, resulting in three general patterns: horizontal being the most common (Fig. 11d-g), oblique (Fig. 11c) and longitudinal (Fig. 11a-b).

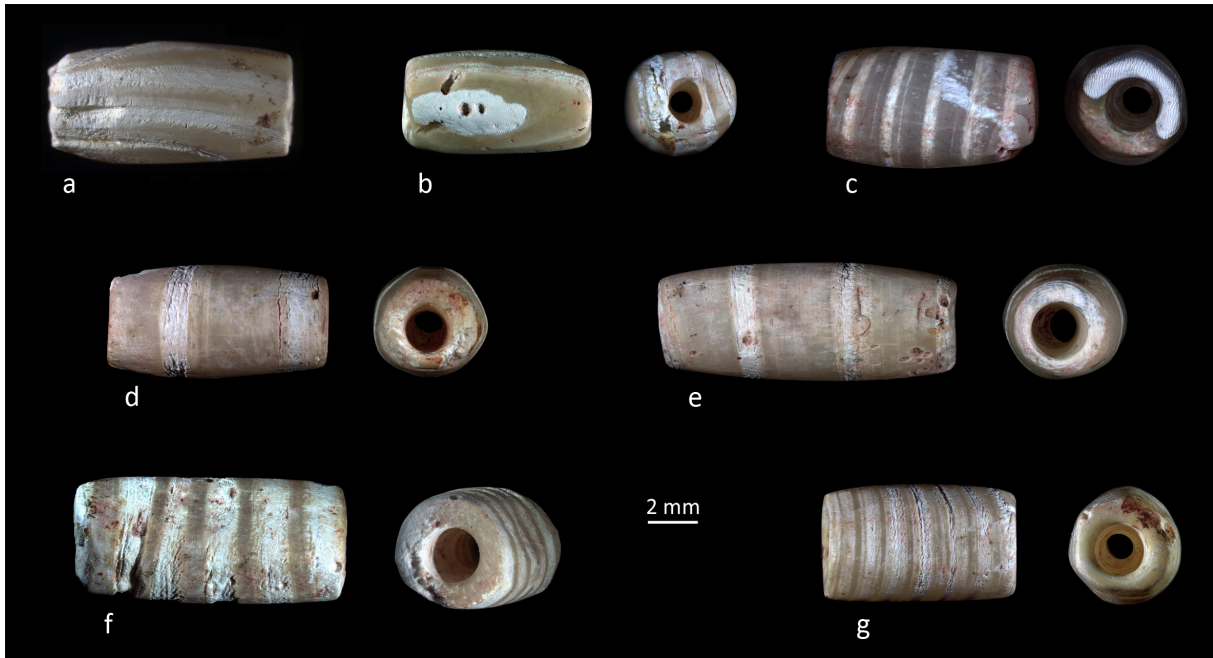


Fig. 11 Examples of the shell tubular beads from the burial: *a* presented in profile and *b-g* face of perforation. (Photos: H. Alarashi, Ba'ja N.P.)

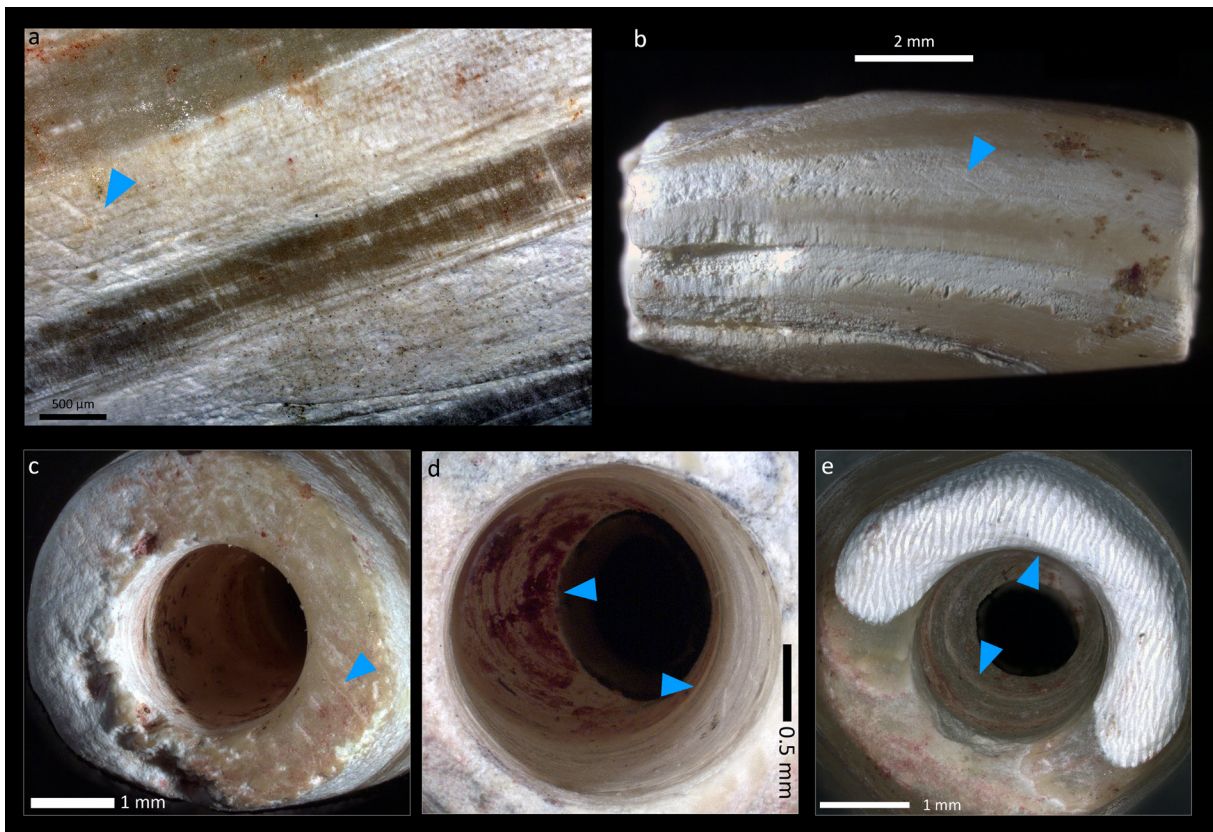


Fig. 12 Technical and use-wear traces on the tubular shell beads: *a-b* deep oblique and longitudinal striations of abrasion (shaping) and/ or polishing (finishing), *c* deep parallel striations of abrasion and/ or polishing on the perforation face, *d* deep concentric drilling striations marked on the wall of the perforation, see also the remains of red ochre inside the striations and on the walls, *e* circular shape of the rim of the drilling at the opening and at the end, with well-marked concentric deep and shallow drilling striations. See also the rounding of the rim of perforations in *c*, *d*, and *e*. (Photos: H. Alarashi, Ba'ja N.P.)

A one-way ANOVA attests that there is a statistically significant difference in length ($F=5.381$; $p[\text{same}]=0.00583$) between groups of beads displaying different banding patterns. Indeed, the results of the Tukey post hoc test ($F=4.576$; $p[\text{same}]=0.004475$) indicate that the beads of the longitudinal pattern are significantly shorter (mean $L=7.30\text{mm}$) than the beads of the horizontal pattern (mean $L=9.72\text{mm}$). No significant difference was observed between the horizontal and the oblique pattern (mean $L=9.13\text{mm}$). These differences can be explained by a techno-economic management of the raw material: when the fragment was not long enough to shape the horizontal (or oblique) pattern, it was shaped differently in a longitudinal pattern, so that the material would not be wasted. The artist might have wanted to vary the patterns to create a more dynamic ornamental composition. Yet there is no correlation between the emplacement of the beads within the ornament and the variability of patterns, which makes the first hypothesis more plausible.

Longitudinal parallel striations (Fig. 12a-b) are observed on the surfaces of the beads indicating their polishing, which corresponds generally to the final stage of the manufacture. Parallel deep striations are also registered on the faces of perforations (Fig. 12c).

In several cases, these striations are interrupted by the circular concentric striations of the drilling stage, indicating thereby that the perforation took place at least after the final shaping of the bead. It is hard to distinguish whether the smooth surfaces resulted from an intentional polishing or from the use of the beads, especially because the regularity of the shapes created from a relatively soft material could be also due to a final polishing.

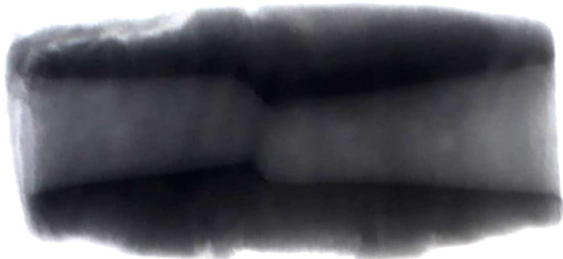


Fig. 13 A micro-CT scan of a shell bead (F.no. 110825.1009) showing the conical tubes and their imperfect alignment. (Photo: B. Demarchi, University of Turin)

All of the shell beads have bi-polar drillings (made from opposite sides) that cross the length of the bead at relatively even distances (Fig. 13). The tubes composing the perforation have sub-conical sections, hinting at the shape of the drilling bit used. They are rarely aligned in the same axis, meaning that when each drilling is virtually prolonged, the tubes are either parallel (Fig. 12e) or slightly crossed (Fig. 12d). Such observations help in evaluating the technical investment and the skills of bead makers.

The outlines of the perforation rims are of a regular circular shape (Fig. 12d-e), and the perforation walls are marked with parallel concentric regular striations (Fig. 12c-e) typical of fast-drilling techniques such as a bow-drill or a pomp drill.

While most of the beads show traces of ochre on their surfaces, many of them have also important amounts of ochre inside the perforation. Similar observations were made from tubular shell beads found at the site in non-funerary contexts (Alarashi a this volume: Fig. 9a). Were the strings used to thread the beads covered with ochre, or is its presence inside the perforation rather due to other actions related to the funerary event? The study of beads from other burials will possibly help to understand the use of ochre for ornamental purposes. The use of ochre during burial rituals is attested in various forms as lumps of ochre, spreading red liquid in collective burials, with bones and artefacts showing traces of red pigment, colouring of human bones or complete colouring of shells such as in the collective Burial CG11 in Room CR17:117 where a cowry was stained red (Gebel and Hermansen 2001; Gebel *et al.* 2019, 2020; Gebel b this volume).

The tubular *Tridacna* beads show low intensity of use represented by the rounding of the edges of the perforations, and the intersectional edge between the face of the perforation with the profile of the bead (Figs. 11g, 12c-e). Scratches and/ or polish are generally more frequent on the faces of perforation than on the profile of the beads. This is likely due to the friction caused by the bead-to-bead alignment in a chain, and to the friction with the string between them. If these beads were used during a lifetime, the wear was not intense enough to completely erase the technical traces, especially the drilling striations inside the perforations, with their circular continuity being still visible.



Fig. 14 Examples of flat and tubular calcite beads: a-c examples of bi-truncated flat beads with lenticular section; d-f examples of tubular calcite beads of a cylindrical type; f use-wear marks: eraser of the drilling striation, thinning and fracture of the walls of the perforation due to friction and incrustation within the perforation of other aligned beads. (Photos: H. Alarashi, Ba`ja N.P.)

Calcite tubular beads (Fig. 14d-e) were manufactured according to the same method as the calcite flat beads. They have use-wear marks on the extremities, represented by a partial obliteration of the drilling striations with a polish or with polish and thinning of the edges of the perforation (Fig. 14f). These marks are known to be produced by a bead-to-bead contact and friction, which is coherent with the chain-like general organisation of the beads that it provokes, sometimes causing the incrustation of extremities into those of other beads.

Flat Beads

A total of seven flat beads were identified, very similar in size (Fig. 20) and all having a truncated sub-oval profile (Fig. 14). Within this burial, they were exclusively made from red calcite. So far, only one similar calcite flat bead was found at Ba`ja, in the multiple Burial CG9 of four subadults (F.no. 110825.850). The same type made from marine shells occur regularly at the site in both funerary and other contexts (Alarashi a this volume: Appendix 1, Alarashi and Benz this volume: Appendix 1).

Compact Spherical Beads

The spherical type is represented by two hematite beads (Fig. 15) similar in size (Fig. 20). The transversal section is sub-circular, and the colour is brownish to dark red. This type is very rare in the region. One comparable bead is known from

the Late Pre-Pottery Neolithic B (Late PPNB) site of Basta, from Loc. B68:13 (F.no. 10835; Hermansen n.d.).² Another very similar parallel that can be mentioned comes from a PPNA context from the northern Levant, a black chlorite spherical bead from Tell Mureybet (Maréchal and Alarashi 2008: Fig. 18.13). Spherical beads of different sizes made from carnelian and agate were also found in a burial of a child at Tell Halula (Alarashi 2014).

Double Perforated Object

An exceptional object is the hematite flat oval plaque with a bilateral double perforation (Fig. 15a-b). Other double perforated stone objects were found at Ba`ja. These were generally made of turquoise (Gebel *et al.* 2020). However, none of these are comparable in the regularity of the shape, the size, and the quality of finishing, especially given the hardness of the stone.

This object was found behind the neck of the child with many disc beads above and below it, and with some beads still sticking to its perforation. Due to this position and configuration, this artefact has been called a “buckle” since its first appearance in the field, a designation that the use-wear analyses confirmed (*cf. infra*).

Multidirectional deep striations are found all over the surfaces of the buckle and the spherical hematite beads. The latter also show impact points and scratches everywhere (Fig. 15i-j). Despite the density and hardness of the material, the buckle was intensively used. The surfaces show shiny polish (Fig. 15a-b,h), very intensive rounding of the edges, and enlargements of the perforations towards the external edges (Fig. 15c-f) in two opposite directions, as if the perforations were under significant tension. These observations support the hypothesis that this object was used as a “spacer” or “buckle” to hang strings of beads behind the neck.

Decorated Ring

The study of the morphometrical attributes of the mother-of-pearl ring appeared as a

² Two other hematite beads were uncovered at the same site in Area A: one of a very amorphous subspherical shape from a burial context (F.no. 20936; Room 28, Loc. 23) and one biconvex rather flat bead (F.no. 5006; Area A2, Loc. 2) (Hermansen 2004, n.d.).



Fig. 15 Hematite elements, types and technological and use traces: *a-h* double perforated pendant, *i-j* spherical beads. (Photos: H. Alarashi, Ba`ja N.P.)

crucial step to understanding the organisation of the ornament, since the first moments of its discovery. The size, the number of the perforations, their distribution, and the shape of the decorated areas were inferred based on measurements and on comparisons with other similar items discovered at the site (*e.g.*, the above-mentioned ring found in the collective Burial DG1, in Area D; Gebel and Hermansen 2001). Nomenclature and convention of the measurements are given in Fig. 16, while the measurement values are presented in Table 3.

In the largest fragment of the ring, one almost complete outgrowth (Outg. I) is

preserved with six perforations (two complete on the ring area, and four on the outgrowth area, three of them broken), and one broken outgrowth (Outg. II) containing two perforations (one complete and one broken). Another small fragment of the ring has a broken outgrowth (Outg. III) with two broken perforations located on the outgrowth area. A total of ten perforations were counted on the preserved fragments of the ring and its outgrowths. The diameter average of the perforations is 2.80mm. The average distance between the two perforations is 3mm. The distance between Outg. I and II is almost the same as the length of Outg. I.

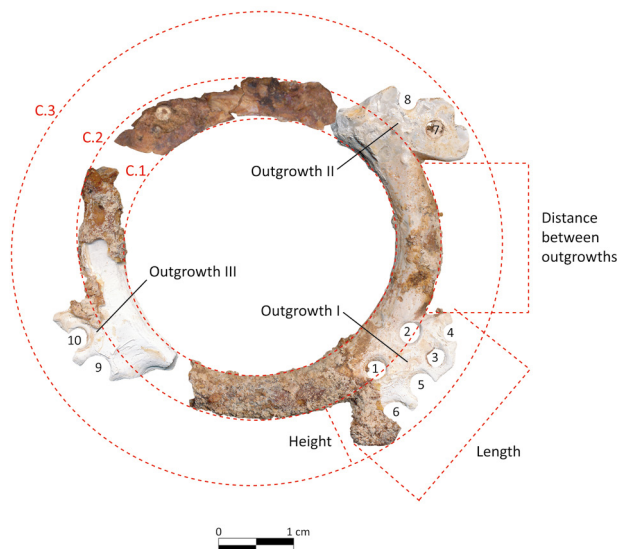


Fig. 16 Nomenclature and convention of measurements used for the study.

Table 3 Detailed measurements and estimations of the MOP ring. Outg.=outgrowth, P=perforation, all measurements are given in mm.

Outg. I P6	3.11
Outg. II P7	2.53
Outg. II P8	2.55
Outg. III P9	3.87
Outg. III P10	2.46
Distance P1 and P2	3.96
Distance P2 and P3	2.53
Distance P2 and P4	3.13
Distance P1 and P5	3.61
Distance P1 and P6	3.33
Distance P7 and P8	2.77
Distance P9 and P10	1.75
Distance between Outg. I and II	20.22
Estimation length Outg. I	20.1
Estimation height Outg. I	8.9
Estimation height Outg. II	8.0
Estimation maximum inner diameter	30.52
Estimation maximum middle diameter	40.68
Estimation maximum outer diameter	60.44
Width ring before Outg. II	5.02
Width ring before Outg. I	5.58

These measurements and the preserved features suggest the following:

- Each outgrowth measures around 22mm length and 8 to 9mm height. This means, a fourth outgrowth can be placed perfectly on the opposite side of Outg. I. A ring with four outgrowths provides equilibrium to the composition with its decorated areas distributed symmetrically, separated one from the other by around 25mm.
- Three outgrowths bear four equidistant perforations, while one has two additional ones on the ring part. The latter might have had a different function than the others. With an additional outgrowth, the possible total number of perforations amounts to 18.
- Based on the preserved shape of the outer edge of Outg. II (the part integrating perforation n° 7) the engraving pattern of the other outgrowths was most likely identical: a denticulated motif consisting in a convex line with equidistant regular deep incisions, probably four, as if the artist wanted to mark a visual separation between the areas of perforations within each outgrowth.

Previous excavations at Ba`ja have revealed a completely preserved ring (Fig. 17, F.no. 30408; Gebel and Hermansen 2001) showing very similar features to those of the ring found in the child's burial: a) four outgrowths with equidistant perforations within each; b) one outgrowth with two additional perforations on the ring portion; c) denticulated decoration pattern of the edges. In two lately excavated burials (BJ19-CR17 [CG11] and BJ19-CR28.2 [CG9]), two cross-shaped mother-of-pearl objects, one multiperforated, have also four crossing branches with denticulated edges (F.nos. 110412, 110414; Gebel *et al.* 2020: Fig. 34). Generally, the denticulated motif is recurrent for the mother-of-pearl items found at the site (Gebel 1988: Fig. 11.6; Alarashi a this volume: Fig. 5y).

The measurements, the distribution of the perforations, the symmetry of the preserved portions, and the presence of strong parallels of emblematic mother-of-pearl items at the site, helped in reconstructing the initial shape of the ring (Fig. 18). It is a large example of a flat decorated type (Alarashi a this volume: Fig. 9), with four outgrowths that expand from the main torus.

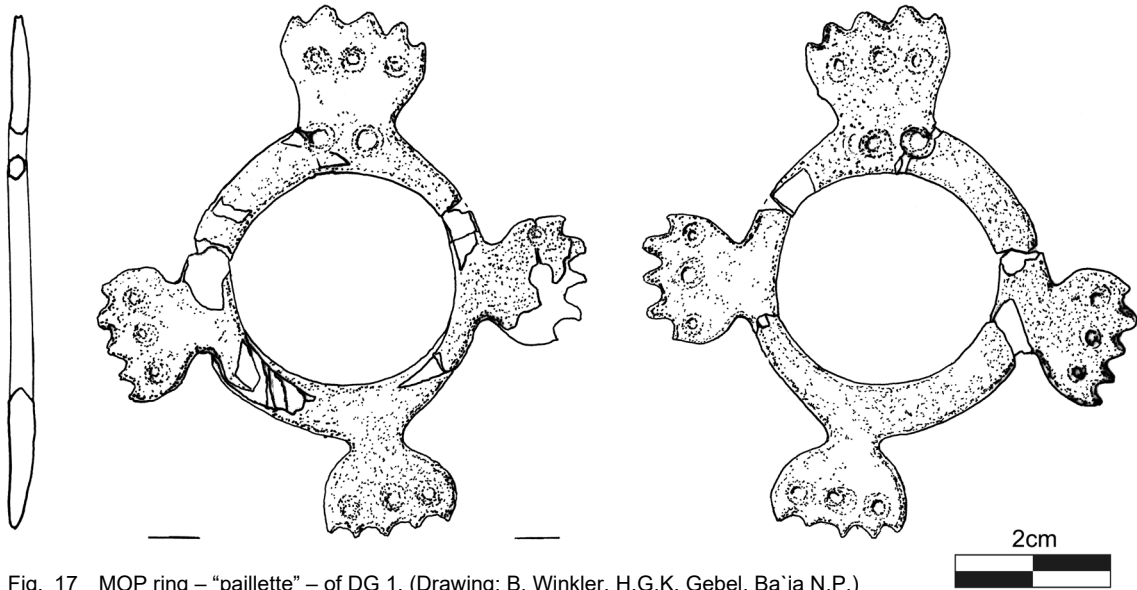


Fig. 17 MOP ring – “paillette” – of DG 1. (Drawing: B. Winkler, H.G.K. Gebel, Ba’ja N.P.)

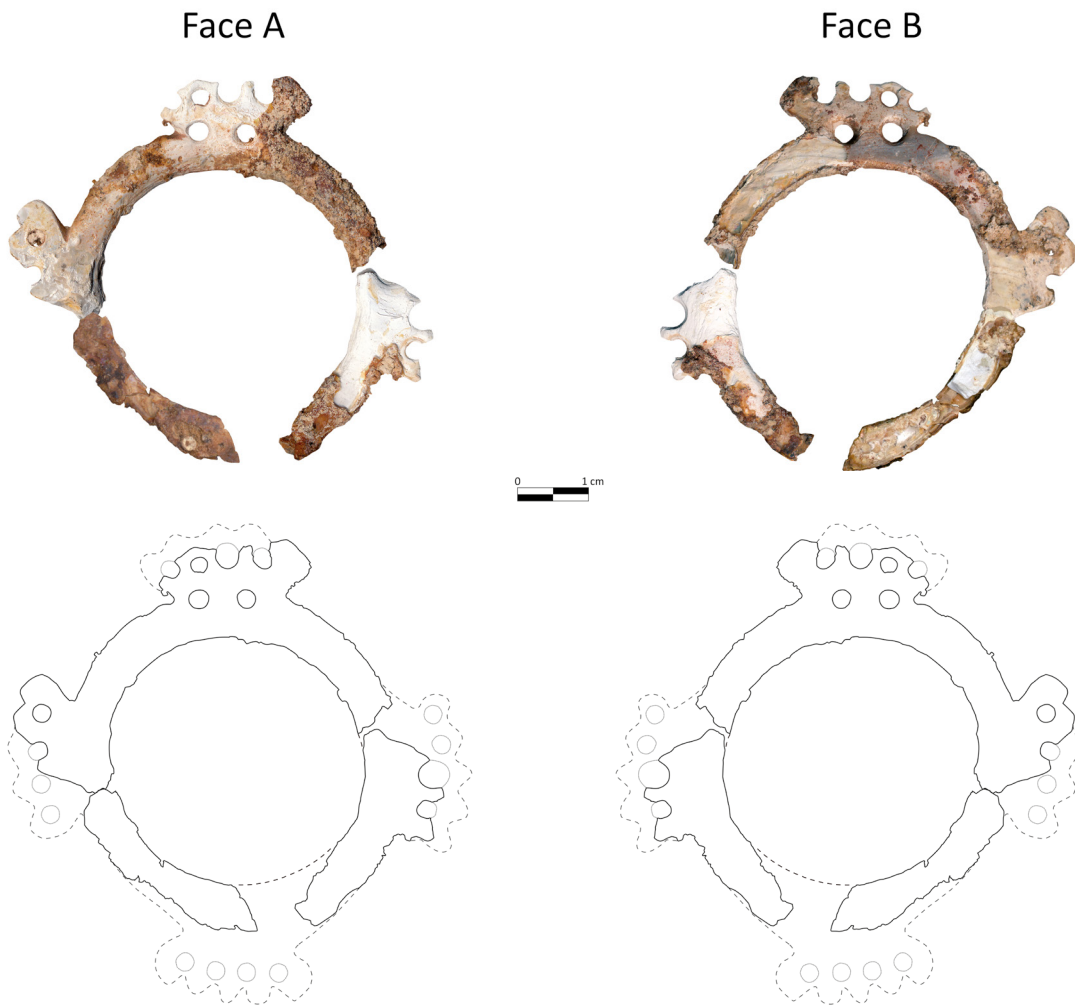


Fig. 18 Flat decorated MOP ring: Faces A and B of the preserved and restored fragments above. (Scans and refitting: H. Alarashi and A. Costes, restoration: A. Costes, drawing of the hypothetical reconstruction: H. Alarashi, Ba’ja N.P.)

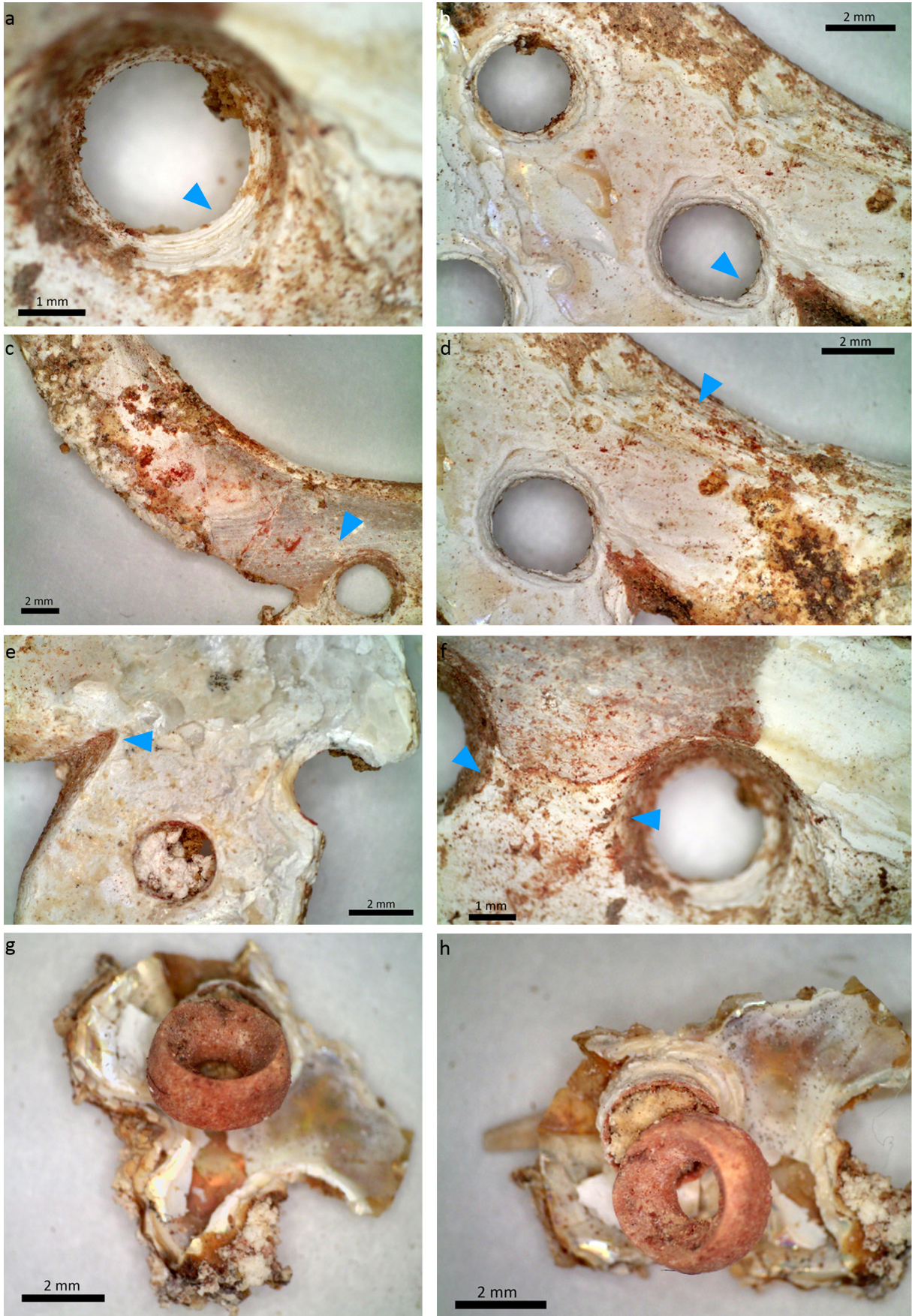


Fig. 19 Traces observed on the deteriorate surfaces of the MOP ring. (Photo: H. Alarashi, Ba`ja N.P.)

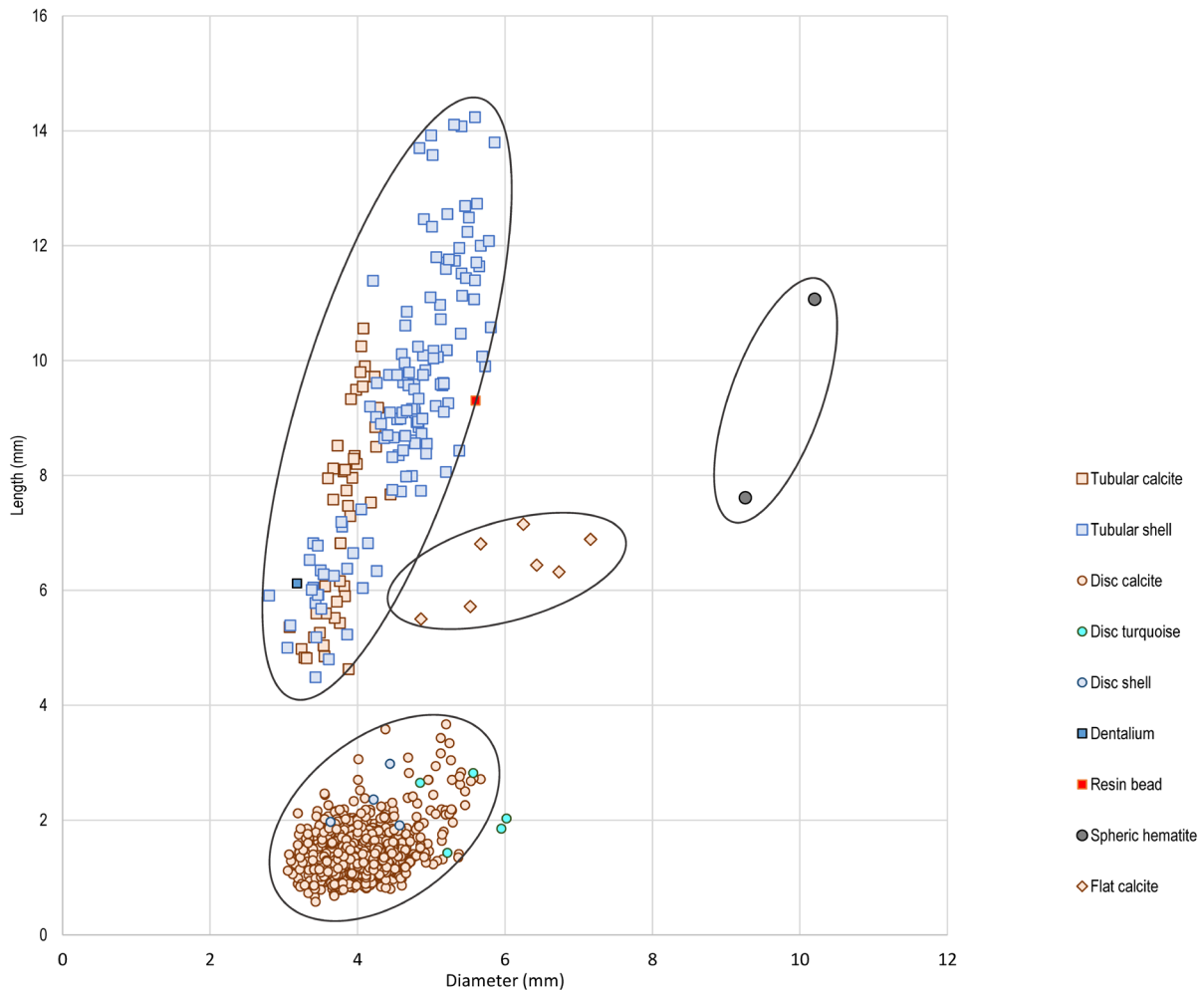


Fig. 20 Proportions of beads according to their types and sizes. Plots of values of all the measured beads from the bead corpus exported to Nice. (Graph: H. Alarashi, Ba'ja N.P.)

The microscopic examination of the ring was done very carefully as the surface was very deteriorated. Manipulating the ring was therefore risky. Despite this state of preservation, technical marks were observed:

- parallel abrasion striation (Fig. 19c) on the convex part to reveal the nacreous surface (Alarashi a this volume: Fig. 8, 1st stage, slab preparation),
- curved striations on the outer and inner (Fig. 19d) circumferences to extract the ring from the slab (Alarashi a this volume: Fig. 8, stages II and III),
- sawing marks on the outer circumference to engrave the denticulated shape of the outgrowths (Fig. 19e), and the concentric striations on the perforation walls from the drilling (Fig. 19a).

The fabrication produced a considerable number of “waste”, especially during

the engraving. The extraction of the inner circumference of the ring would have produced a relatively large piece of mother-of-pearl (~30mm diameter), with which it is possible to create a range of other objects: buttons, small rings of the simple flat type, *etc.* (Alarashi a this volume: Fig. 5; Benz *et al.* this volume: Figs. 31, 114).

Use-wear analyses were inconclusive because of the poor preservation of the ring. The upper layers of the mother-of-pearl have disappeared almost completely in some areas. It was therefore not possible to decide whether the presence of enlargements on the circumferences of some perforations (Fig. 19b), or depressions between the perforations (Fig. 19f) were due to frictions or tension of the string on these areas. Use-wear analyses made on other rings and mother-of-pearl items from the site show, however, that when multiple perforations are present, relatively intensive wear marks were

observed, meaning that these perforations were functional and not merely decorative. In the case of the child's ring, beads were still stuck to the upper layers of the mother-of-pearl ring at the area corresponding to the perforation. An organic (?) material with ochre residual is still imprisoned inside the perforation of the ring and the bead. It might have been the remaining part of the string.

Morphometric Analyses

The values of the maximum diameter and length of beads were plotted per type and material in Fig. 20. Although the typological families (disc, tubular, flat, compact beads) are clearly distinguished by their morphologies, it is worth noting the general homogeneity of the elements regarding the global size, and more particularly regarding the diameter of the objects. For over 1500 disc and tubular beads, the diameter ranges between 3 and 6mm. The variability is more important for the lengths' values of the tubular beads, especially for the tubular shell beads. Those of a length higher than 11mm were shaped according to a horizontal pattern of the growth lines (*cf. supra*). The oblique or longitudinal patterns occur for shorter specimens. Their mean length is 8.5mm, with only a few items being longer than 10.5mm. This is also the case for tubular shell beads found in other burials. The longitudinal and oblique patterns only occur for short

specimens. If the relation between the pattern of the growth lines and the length of the bead is due to the size of the shell fragment from which these beads were extracted, two suggestions can be made:

1. the shell fragments were longer than they were wide, thus providing the possibility to manufacture long beads with a horizontal pattern,
2. beads with oblique and longitudinal patterns were made from remaining shell fragments.

The size of three main types was examined: the calcite disc beads, the calcite tubular beads, and the shell tubular beads. The metric data (Table 4) show low values of standard deviations (SD) of the diameter and of the perforation for all the types, meaning that the diameter and the diameter of perforation were standardised for all the types, and per type. In the case of disc beads, even the length values are highly standardised (low SD), meaning that their creation required significant control.

The regularity of the shape of the disc beads was examined by calculating the degree of circularity (*Script ImageJ*). A perfect ellipse (a circle) has the value of 1. The values of the disc beads (n=1419) have an average of circularity of 0.890 (maximum=0.908, minimum=0.773) and a very low standard deviation of 0.012. In other words, the disc beads have very regular circular shapes that

Table 4 Metric values of the main types found in the burial (GN).

Beads	Metric Data (mm)	Length	Diameter	Perforation
Calcite disc n=1492	Maximum	3.67	5.67	2.302
	Minimum	0.58	3.056	0.944
	Average	1.423	4.045	1.546
	Standard deviation	0.347	0.391	0.223
Calcite tubular n=46	Maximum	10.56	4.45	3.12
	Minimum	4.63	3.08	1.4
	Average	7.26	3.80	1.98
	Standard deviation	1.75	0.30	0.41
Shell tubular n=126	Maximum	14.24	5.86	3.06
	Minimum	4.49	2.8	1.24
	Average	9.34	4.68	2.07
	Standard deviation	2.27	0.70	0.34

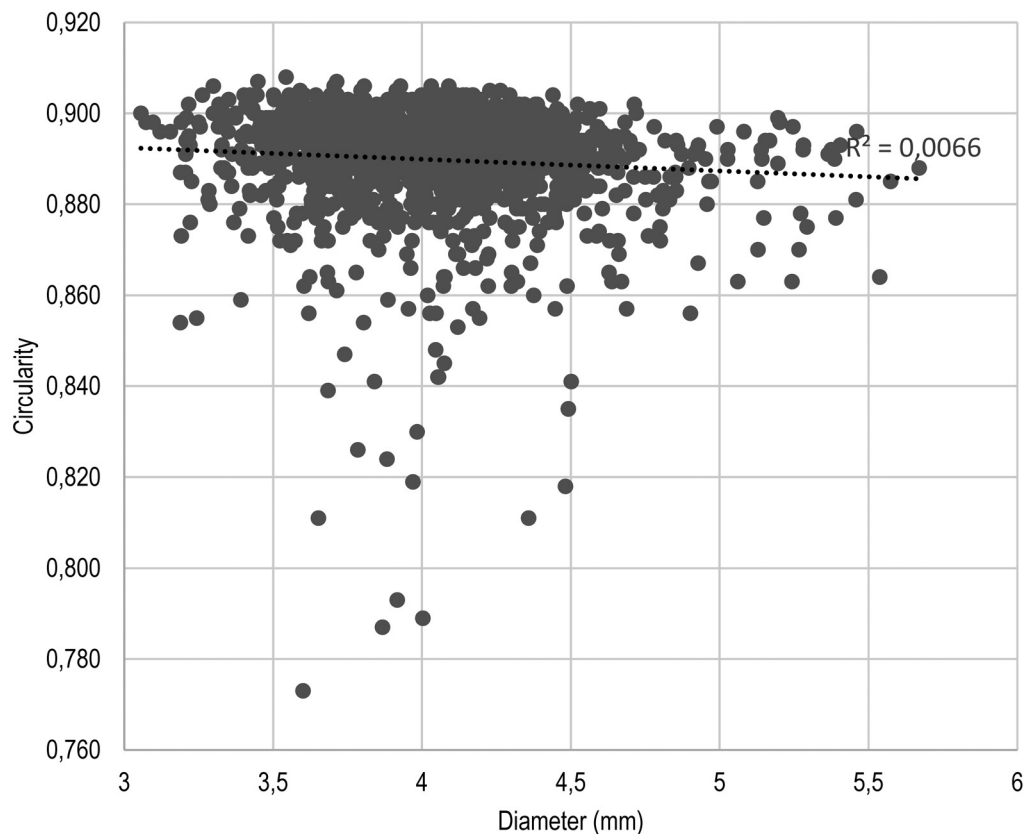


Fig. 21 Plot of the diameter and degrees of circularities of the calcite disc beads. (Graph: H. Alarashi, Ba'ja N.P.)

are very hard to obtain, if these were grounded manually and singularly (one by one).

There is no correlation between the degrees of circularity and the diameters of the disc beads (Fig. 21). The regularity of circularity applies to all the sizes. However, some discs having small diameters that range between 3.5 and 4.5mm are less circular than others. Both aspects (the diameter and the degree of circularity) are likely due to technical issues, probably to breakage during the final stages of batch or serial abrasion (Fig. 10c).

The Reconstruction of the Necklace

Because of the collapse of the ornament, the initial organisation of the beads and of the rows of beads was not intact in all parts. Therefore, in order to identify the type of the ornament and its organisation, all the available information – field observations, metrical analyses, mathematical estimations, results of the beads' study and logical deductions – were mobilised. The results revealed that the assemblage of

beads corresponds to an exceptional necklace of highly sophisticated organisation.

The Role of the Mother-of-Pearl Ring

The mother-of-pearl ring was the masterpiece of the necklace from which rows of strung beads have spread to adorn the chest and neck of the child. The ring also divided the necklace into two even left and right sides.

The orientation of the outgrowths of the ring was decisive for understanding the way the ornament was displayed, for determining the number of rows, and their lengths respectively. Two orientations were possible: in a Greek (+) or a Saint Andrew's cross (x). The first is the most plausible because:

- one of the outgrowths has two additional perforations suggesting the direction of orientation of the ring in an up-right position. The position of the ring when discovered confirms this orientation (Fig. 3).
- If the rows of the necklace spread from the ring were displayed in a St. Andrew's

cross orientation, the natural (and logical) path of the rows would be around the shoulders and below the arms, reaching the back of the child. However, the concentrations of beads were located around the neck on the chest, and none of the beads was found on the lateral side of the torso below the arms.

- The concentration of beads around the neck and on the upper part of the chest but also behind the neck and around the occipital bone, in and beneath the mandible and to a lesser extent around the facial bone of the skull, argue in favour of displaying the necklace around the neck and the chest, and against a display around the torso.

The Greek cross orientation is also supported by the discovery of several large mother-of-pearl items at the site. Their shapes, engravings and perforations indicate this orientation (Benz *et al.* 2020: Figs. 4-5).

Configurations According to the Number for Rows

Presuming that the outgrowths were oriented in a Greek cross position and that the perforations of the ring were used to fix the rows of beads (as departure points of the rows), and given the very high number of beads sufficient to fill tens of strings (*cf.* below), two plausible configurations of the necklace can be proposed:

1. A constrained configuration: it considers the 18 perforations of the ring, thus proposing 18 rows, nine to the left and nine to the right, graduated in length, and all gathered behind the neck using the stone buckle (found behind the child's neck, *cf.* Fig. 1h-i). The use of the perforations of the (unpreserved) outgrowth, the one opposite to Outg. I (Fig. 18), to hang rows departing towards the neck forces the ring to tilt or incline forward, unless the latter is stitched to a support (cloth?), and unless these four rows were very long and moved aside (two to the left and two to the right) beyond the other rows and maintained fixed. Otherwise, they will hamper the visibility of the ring and of the other rows.
2. A "free" configuration: it allows a display free from fixations or special arrangement ensuring an optimal visualisation of the ring and the other rows. It is based on the use of 14 perforations, those of the main (Outg. I) and lateral outgrowths, *i.e.*, 14

rows – seven to the left and seven to the right. Rows spread from these perforations can be gathered comfortably behind the neck. The perforations of the bottommost outgrowth might have been used to hang vertically short strings of beads, or to stitch the ring to a cloth.

The collapse of the necklace after the decomposition of organic materials makes it impossible to confirm one of these configurations. Nevertheless, the second configuration seems more convincing as it doesn't require further adjustments for an already complex necklace. For this reason, the reconstruction adapted the free configuration (*cf.* below).

The Total Length

The rows were distributed between the ring and the stone buckle. The position and length of each row was determined by the ring perforation to which it was fixed, meaning that the lengths of rows gradually increased going from the central perforations of Outg. I towards the lateral ones.

In order to estimate the length of each row, the total theoretical length of the ornament was calculated (Table 5). To do so, the length (or thickness in the case of disc beads) of more than 65% of all beads was used to estimate the length of the unmeasured beads (GS). Table 6 details the estimations of length per type and material, using the basic metric data and the results of the total length measured and estimated (average, minimum and maximum) in mm, cm, and m. The formulas applied:

- Total length (average): length measured beads + (n unmeasured beads * average length of measured beads).
- Total length (minimum): length measured beads + (n unmeasured beads * average length measured beads - (2*Standard deviation measured beads)).
- Total length (maximum): length measured beads + (n unmeasured beads * average length measured beads + 2*Standard deviation measured beads).

The total length of the necklace when all the beads found in the burial are aligned tightly in a chain-like arrangement is impressive. The minimum estimated is almost five meters, the maximum is over seven metres, and the average

Table 5 Estimations of the total length of the ornament through the measurements of the lengths of beads and the estimation of the unmeasured beads. C=circular, D=disc, B=bead, T=tubular, O=oval, F=flat, DPP=double perforated pendant, S=spherical.

Type	Total n	Beads						Unmeas.	Total L.	Total L. Estimations		
		Measured	Ave.	StD	Min.	Max.	Measured		Average	Minimum	Maximum	
CDB calcite	2264	1492	1.42	0.35	0.58	3.67	772	2122.57	3220.84	2685.22	3756.47	
TB shell	232	126	9.34	2.27	4.49	14.24	106	1177.18	2167.51	1685.41	2649.60	
TB calcite	66	46	7.26	1.75	4.63	10.25	20	334.00	479.22	409.19	549.25	
TB resin	2	1	9.31	0.00	9.31	9.31	1	9.31	18.61	18.61	18.61	
Conus discs	4	4	2.31	0.49	1.91	2.98	0	8.22	8.22	8.22	8.22	
ODB turquoise	5	5	2.16	0.57	1.43	2.82	0	10.78	10.78	10.78	10.78	
FB	7	7	6.40	6.40	5.50	7.15	0	44.83	44.83	44.83	44.83	
DPP	1	1	29.13	0.00	29.13	29.13	0	29.13	29.13	29.13	29.13	
SB hematite	2	2	9.34	2.45	7.61	11.07	0	18.68	18.68	18.68	18.68	
Dentalium	1	1	6.12	0.00	6.12	6.12	0	6.12	6.12	6.12	6.12	
TOTAL	2584	1685	Millimetres				899	3760.82	6003.94	4916.18	7091.69	
							Length in metres	3.7608	6.0039	4.9162	7.0917	

is around six metres. To estimate the lengths of the rows, the average of the total length was considered: 6.0039, rounded to 6 metres.

Estimation of the Rows' Lengths and Readjustment of Their Number

In order to obtain a reliable estimate of the lengths of the rows within the volume of a necklace that fits a child's body (in a standing position), we considered the range of standard sizes of children of both sexes between the age of seven and nine years. The measurements of the upper body were obtained from the measurement charts of AFNOR³ (Table 6).

Based on the measurements of neck, shoulder breadth, and the distance from the 7th cervical vertebra to waist (front and back), it was defined that the maximum spread of the necklace in width (the distance between the lateral exterior rows) and length (between the buckle and the fourth outgrowth of the ring) should not be greater than 30cm each.

Several calculations were made considering 14 rows (seven on each side) in order to obtain, at once, enough length to integrate all the beads to fit an eight-year child's body of a normal size. Even when the maximum

possible child's size (C, in Table 6) was considered, all the estimations gave inappropriate results when they were based on 14 rows. For example, the total length reached with 14 rows was less than 4.5m (4481.81mm), and the integrated beads were only 2138. This means that more than 1.5m were needed to integrate the remaining 446 beads (all types). It was therefore necessary to increase the number of rows and to place them in the centre of the necklace. Indeed, the configuration with only 14 rows leaves an important empty space in the areas corresponding to the front of the neck and the upper chest. This contradicts observations made in the field as these two areas are, precisely, those most densely covered with beads, showing several alignments that could be sections of several rows.

Three additional rows of gradual lengths were added to the upper part of the necklace (Table 7). However, we lack indications of whether these were linked or not to the ring in this case to the main outgrowth (Outg. I). The presence of additional perforations in this outgrowth is an argument in favour of the connection of the upper rows (R1, R2, R3) to the ring. Nevertheless, the possibility of having rows of the necklace not connected to the ring cannot be excluded. Moreover, most of the tubular shell beads, especially the big ones, were discovered in large quantities around the neck, a privileged zone of the body used to exhibit remarkable beads that show variable patterns of natural strips (Fig. 11). They probably provided an

3 French Standardization Association: http://data.over-blog-kiwi.com/0/67/75/45/201308/ob_76318e_tableaumenturationsenfant-afnor87.pdf.

Table 6 AFNOR measurement chart (unless otherwise stated in cm) of actual children of both sexes between seven and nine years' old. T=thin, N=normal, C=corpulent.

		Girl			Boy		
		7	8	9	7	8	9
Years		7	8	9	7	8	9
Height		120	126	132	120	126	132
Bust circumference	T	56	58	60	58.3	59.8	62.1
	N	62	64	66	60.2	62	64.6
	C	68	70	72	62.7	64.9	67.7
Shoulder breadth	T	23.1	23.8	24.5			
	N	24.3	25	25.7			
	C	25.5	26.2	26.9			
Back breadth	T	24.8	25.6	26.4	26.5	27.5	28.5
	N	26.3	27.1	27.9	27	28	29
	C	27.8	28.6	29.4	27.6	28.6	29.7
Neck circumference	T	25.4	26	26.6			
	N	26.3	26.9	27.5			
	C	27.2	27.8	28.4			
Shoulder's length	T	9	8.6	10.1	9.4	9.9	10.3
	N	9.5	10	10.5	9.5	10	10.4
	C	10	10.4	10.9	9.7	10.1	10.6
7th cervical vertebra to waist (front)	T	34.3	36.4	38.5			
	N	34.8	36.9	39			
	C	35.3	37.4	39.5			
7th cervical vertebra to waist (back)	T	27	28.2	29.4	28	29.2	30.3
	N	27.4	28.6	29.8	28.4	29.5	30.6
	C	27.8	29	30.2	28.8	29.9	31
Collar size	T	28.6	29.3	30	28.2	28.9	29.7
	N	29.5	30.2	30.9	28.7	29.4	30.2
	C	30.4	31.1	31.8	29.2	30	30.8
Shoulder's inclination (slope)	T	23.1°	22.8°	22.6°			
	N	22.9°	22.6°	22.4°			
	C	22.7°	22.4°	22.2°			

interesting visual effect, *i.e.*, a certain dynamism in the continuity of the rows. Connecting the rows to the ring would weaken these effects, as the attention would be more drawn to the ring. A good compromise that allows highlighting these exceptional beads would be the creation of some discontinuity, namely, disconnecting the upper rows from the ring.

Whether the upper rows were connected or not, the best number of rows to exhibit and organise the ornament is 17. For the reconstruction we chose the scenario of three separated chains connected to the buckle, and 14 rows, seven on the left and seven on the right side, connected to both the ring and the buckle (Fig. 22A).

Table 7 Estimations of lengths of the rows (cm) and the number of beads and types of beads to be integrated. For abbreviations see Table 5.

Rows		Right Side				Left Side							
		CDB calcite	TB shell	TB calcite	Total	CDB calcite	TB shell	TB calcite	Total				
R1	n	100	24	10	134	50	12	5	67	50	12	5	67
separated	length	142.19	224.22	71.876	438.29	71.096	112.11	35.938	219.15	71.096	112.11	35.938	219.15
R2	n	110	24	10	144	55	12	5	72	55	12	5	72
separated	length	156.41	224.22	71.876	452.51	78.206	112.11	35.938	226.26	78.206	112.11	35.938	226.26
R3	n	110	26	10	146	55	13	5	73	55	13	5	73
separated	length	156.41	242.91	71.876	471.2	78.206	121.46	35.938	235.6	78.206	121.46	35.938	235.6
R4	n	152	27	6	185	76	13.5	3	92.5	76	13.5	3	92.5
connected	length	216.24	252.25	43.125	511.62	108.12	126.13	21.563	255.81	108.12	126.13	21.563	255.81
R5	n	182	25	6	213	91	12.5	3	106.5	91	12.5	3	106.5
connected	length	258.92	233.57	43.125	535.61	129.46	116.78	21.563	267.81	129.46	116.78	21.563	267.81
R6	n	222	24	5	251	111	12	2.5	125.5	111	12	2.5	125.5
connected	length	315.82	224.22	35.938	575.99	157.91	112.11	17.969	287.99	157.91	112.11	17.969	287.99
R7	n	272	21	5	298	136	10.5	2.5	149	136	10.5	2.5	149
connected	length	386.96	186.85	35.938	609.75	193.48	93.427	17.969	304.87	193.48	93.427	17.969	304.87
R8	n	312	21	5	338	156	10.5	2.5	169	156	10.5	2.5	169
connected	length	443.86	186.85	35.938	666.65	221.93	93.427	17.969	333.33	221.93	93.427	17.969	333.33
R9	n	372	20	5	397	186	10	2.5	198.5	186	10	2.5	198.5
connected	length	529.22	186.85	35.938	752.01	264.61	93.427	17.969	376.01	264.61	93.427	17.969	376.01
R10	n	432	20	4	456	216	10	2	228	216	10	2	228
connected	length	614.58	186.85	28.75	830.18	307.29	93.427	14.375	415.09	307.29	93.427	14.375	415.09
n total		2264	232	66	2562	1132	116	33	1281	1132	116	33	1281
length total		3199.3	2148.8	474.38	5822.5	1599.7	1074.4	237.19	2911.3	1599.7	1074.4	237.19	2911.3

Composing the Rows, Placing the Beads

For the reconstruction it was imperative to understand the patterns of distribution of the bead types that made up the main parts of the necklace: the disc beads, the shell tubular beads, and to a lesser extent, the calcite tubular beads. To estimate the number of beads per type to be integrated within each row, the total number per type was divided by the total number of rows, and the result was adjusted (increased or reduced, Table 7) based on the general distribution of beads within the ornament area, knowing that the red disc beads were present in all the rows and in all parts while the tubular shell beads, and to a lesser extent the calcite tubular beads, were more concentrated in the middle around the neck.

The arrangement and rhythm of integration of beads per type was based on the patterns of arrangements observed in the field, particularly on the alignments found *in situ* (e.g., Fig. 1h-o).

The other 22 beads representing different types and materials (four *Conus* and five turquoise disc beads, seven flat calcite beads, two spherical hematite beads, two resin beads, one *Dentalium*: Table 3) had to also be placed within the necklace. These beads make a total of 12.70cm (average), a length to be added to the six meters established for the necklace integrating only the main types. In addition to observations made in the field regarding their position, the functional, visual, and typological criteria were considered in order to place these beads within the necklace. The five turquoise disc beads were distributed in important places in order to ensure their visibility as they were quite small, yet very valuable and exotic. Their emplacement in a strategic place would also provide dynamic visual effects, as it punctuates the necklace with different colours. The turquoise and dark brown colours contrast with the dominant colours red and white. The flat beads are typical of the Late PPNB period in the Levant. Their occurrence within the assemblage

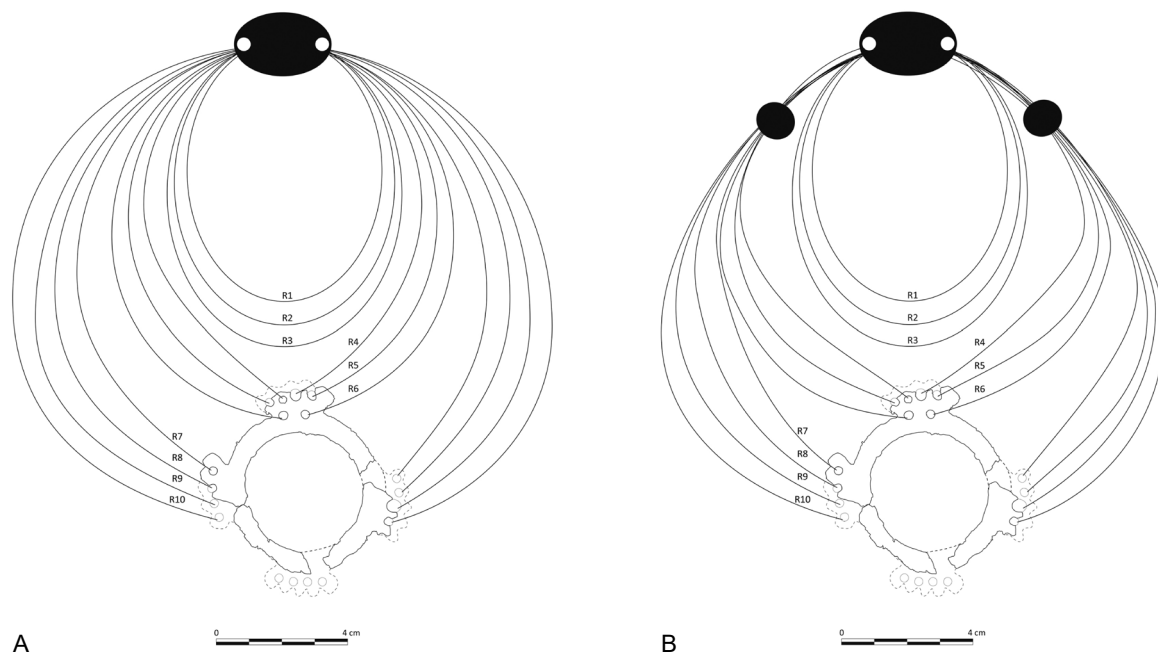


Fig. 22 A The structure of the necklace between the MOP ring and the buckle, and B its display when exterior rows (R4 to R10) are gathered with the spherical beads. (Graph: H. Alarashi, Ba'ja N.P.)

in reddish calcite is – with one single exception (F.no. 110825.850, Burial CG9) – exclusive to the child's Burial CG7. As for the tubular resin beads, it is still not clear whether their importance was due to the nature of the material, the colour, or other considerations.

The spherical hematite beads, beside the contrast created by their dark colour, were most likely employed to canalise the rows of beads; to start gathering them before reaching the buckle. The size and the perforations of these two beads are larger than any other type, and the rims and the walls of perforations show intensive use-wear marks, although it is not possible to determine whether these traces were the result of one or several strings rubbing inside the perforations. These beads also show impact points and scratches all over the surfaces, which is to be expected due to their roundness, and as they were part of a complex dense composition. However, similar intensity of use-wear was not observed for the calcite disc beads and tubular shell beads that were also part of the same complex composition. Irrespective of whether these beads served the function of “row gatherer” or not, the presence of these unique items within such a complex necklace composed of many rows makes a lot of sense. Their emplacement at the level of the shoulder would allow adjusting the size of the necklace (for instance reducing the horizontal

breadth to best fit the neck and shoulders of the child). It is worth reminding that these two beads were found in the same zone (Fig. 1j-k), on both sides of the *manubrium*, a position that, in addition to their possible implication in the up-cited function, corresponds with their values. It is not possible to estimate how many strings were introduced inside these beads. At the same time, it is not necessary that the strings of several rows passed inside the perforation, as the gathering of the rows can be made through simple discreet knots at the level of these beads. The possibility of gathering all the rows departing from the ring, or at least the exterior ones (R10 to R4), should not be excluded (Fig. 22B).

The buckle found behind the neck of the child was made from the same dense and resistant hematite as the spherical beads. The very intense use-wear that has deformed the original shape of the perforation rims on this buckle indicate the tension exercised on each extremity. Hence, it is reasonable to think that the use of such material might have been precisely intended to serve certain functions that other softer beads cannot serve. Finally, the use of four *Conus* discs and the *Dentalium* bead that were identified after the excavation, is hard to interpret. Their low number and small sizes would hardly provide a visual effect, despite their white colour that could have motivated their use.



Fig. 23 The final physical reconstruction of the necklace with tubes of black foam as substitutes for the beads which were too poorly preserved to be displayed in the museum. (Photo: A. Costes, Ba'ja N.P.)

The weight of the necklace including the beads, the buckle, and the ring, is estimated to an average of 192.23g, a minimum of 159.57g and a maximum of 226.50g. The use of strings corresponding to an average of 6m length was not estimated as we lack information about the nature of the strings, and whether or not they were treated by some substance which would influence their weight. If the necklace was only composed of these elements, the beads, and the

strings (supposing that beads from perishable materials were not used), its total weight might have not reached 500g – the double of what was estimated above.

From Theory to Practice

The real reconstruction of the necklace (Fig. 23) has respected the lengths of rows indicated in Table 8, with added margins to each extremity

for the attachments. These margins were also necessary to distribute the uncommon beads (turquoise, flat beads, *etc.*).

A specific type of string (Costes and Fischer this volume: Appendix 1) was used to thread the established combinations of beads. Each string was attached to a carton ring having the identical dimensions and shape of the original one. This was fixed on a rectangular spongy 50x50cm platform, a material especially chosen by the conservators.

The reconstruction started row by row – the right section first, then the superior three rows, and finally the left section. Well-preserved beads were prepared and displayed on a large table in order to be strung. Unpreserved or fragile beads were not strung, but their lengths were considered through the integration of plastic tubes that were removed when the necklace was ready for public exhibition (Fig. 23). Bead threading started respecting the order of appearance of beads in the field, which was problematic because – as mentioned above – an important part from the right side had collapsed onto the left one, and the beads from both sides were probably mixed. Therefore, the order of appearance of the beads does not necessarily reflect the original position. Nevertheless, following the order of appearance assures, at least, a certain degree of authenticity, insofar as the needed types for the combinations were available through this order. If this order would not have been respected, the reconstruction would have been arbitrary.

The three upper rows were not attached to the (fake) ring, nor to the buckle. The joining knot of their attachment was hidden however under the buckle. This decision was made in order to allow the conservators to intervene when required, on different parts without decomposing the whole necklace.

Additionally, it was decided not to pass the strings from R4 to R10 inside the spherical hematite beads, in order to avoid damage and the possible pressure, because one of these beads is fragile, and has a small fracture on the perforation rim. The choice was to only gather the sixth and seventh rows from each side, which was completely arbitrary and only done with the aim to showcase the potential function of this type of beads. During the reconstruction it became necessary to adjust the number of beads for the left side of Rows 8 and 10 to achieve identical lengths on both

sides. Therefore the hypothetical Row 3 of the model (Fig. 22) was removed.

Discussion

The results obtained from both, the beads' and the necklace's levels, show high technological and creative investments. Other excavated burials have revealed rich ornamental finds that show differences with the child's necklace in regard to the choices of types and materials (Benz *et al.* 2020, 2023, this volume). These assemblages appear as spectacular as the child's necklace, but they still need to be characterised and investigated. Thus, future in-depth comparisons are expected to bring new insights regarding social status, identities, and more broadly the symbolic behaviour of the community of Ba`ja. Meanwhile the focus in this discussion will remain on the child's necklace, while considering general aspects regarding the ornamental practices at Ba`ja and the Levant.

A Bunch of Attractive Exotic and Local Raw Materials

Among the identified materials used for the necklace, mother-of-pearl (*Pinctada margaritifera*) is attested elsewhere at the site, occurring as valves fragments, worked slabs and also debris (Alarashi and Benz this volume). In a recently excavated domestic context, a fragment of a fossilised *Tridacna* with contrasted growth lines (measuring approximately 2x2cm), represents so far the only raw specimen of the material employed for hundreds of beads for the necklace, and other hundreds for ornaments discovered in other burials (Gebel *et al.* 2019, 2020; Benz *et al.* this volume). This means that for the materials used for the necklace, there is only evidence of raw marine valves. Unworked turquoise, red calcite or fossil resin do not occur at the site. However, other raw materials, such as copper-based minerals (chrysocolla, malachite), hematite, and carnelian, in addition to unpierced or unfinished marine gastropods were discovered in several archaeological contexts (Alarashi and Benz this volume: Appendix 1). Except for hematite, beads of these raw materials also occurred in other burials and contexts at Ba`ja (*e.g.*, Benz *et al.* 2019, Alarashi a this volume: Appendix 1, Alarashi and Benz this volume: Appendix 1). The same materials are mentioned for other sites in the region (*e.g.*, Hauptmann 2004; Hermansen 2004, n.d.; Critchley 2007;

Maier 2008; Spatz *et al.* 2014; Thuesen and Kinzel 2018).

The *Pinctada margaritifera* species used for the ring originated from the Red Sea. The turquoise likely originated from one of the sources in the Sinai Peninsula (Hauptmann 2004; *cf.* Gerlitzki and Martin this volume). The hematite and the reddish calcite were probably available from local sources within the same mineral environment of the site, or from somewhere else in the region of Petra (Hermansen 2004: Fig. 1). As for the marine and resin fossils, the sources are unknown. The diversity of materials used for the necklace thus reflects the wide range of accessibility to local, regional, and supra-regional sources by the community of Ba`ja. This would be true if all the materials were directly procured from their sources and transformed at the site. However, importation of finished beads should not be excluded. Thus, the acquisition of exotic materials could have been possible by displacements of individuals from Ba`ja to the mineral, fossil, and aquatic sources, or by inter-community exchange systems of raw materials or final products. In all cases, the necklace appears as the result of important socio-cultural and economic investment implying sustained, operational circulation networks, probably similar to those responsible for the arrival of turquoise and cowry shells from Sinai and the Red Sea towards the northern Levant (Alarashi 2016; Alarashi *et al.* 2018).

Where is the Workshop?

There is no direct information about whether the elements of the necklace were manufactured at Ba`ja or imported from elsewhere. It is neither clear whether they were assembled together at the village, nor if the necklace was imported as a complete final product. However several considerations provide arguments in favour of bead processing at the site.

The technological study shows that the elements were crafted applying complex technological processes composed from at least three manufacturing stages: shaping, drilling, and finishing. The implementation of each stage requires the application of, at least one technique using specific tools. Depending on the type, the size, and the raw material, the tools involved in the shaping stage and that are attested within the archaeological records, would include grinding stones (abrasion: stone and shell beads), sharp-edged blades (sawing: mother-of-pearl, calcite,

and shell beads) and/or hammers (fragmentation by knapping: shells, hematite, turquoise...). The drilling stage involves drilling tools of parallel sides and of varied length reaching up to 8-10mm. The maximum diameter should not exceed 3mm for the long bits (>10mm long), and 2mm for short ones (<10mm). These were needed to drill the tubular, flat and the spheric beads. Short drilling bits (Groman-Yaroslavski *et al.* 2013) would have also been useful for disc beads, or for the perforations made on the mother-of-pearl ring. The finishing stage would employ fine-grained grinding stones and/or other semi-rigid supports such as leather. Except for long drilling tools not identified at the site (Purschwitz 2017), all others would be easily accessible to the people living in Ba`ja and would compose part of the artisans' tool kits. The setting of the village itself within sandstone mountains offers a very interesting mineral environment where abrasion and polishing work can be performed. The remains of sandstone ring workshops uncovered in many buildings testify to such activities (Gebel *et al.* 2017).

Although use-wear analyses of specific tools have yet to be completed, the involvement of part of the inhabitants of Ba`ja in bead-making activities cannot be excluded, when one considers the presence of unworked minerals and shells, preforms, or unfinished beads. In fact, Ba`ja provides clear evidence regarding the manufacture of mother-of-pearl ornaments (Alarashi this volume, Alarashi and Benz this volume), and it seems very probable that the ring of the necklace was designed and created at the site. Its creation implied certainly the experience of a skilled artisan; the transformation of such a delicate material into a complex sophisticated shape and size represents a big technological and artistic challenge. The assumption that its manufacture took place at Ba`ja suggests that the whole necklace was assembled there too. Consequently the number of beads, their types, the length of rows as well as their size – in other words, the whole design of the necklace was probably determined by the attributes of the ring.

Did the manufacture of the beads take place at Ba`ja as well? Evidence of a workshop has never been attested at the site, *i.e.*, a space of artisanal activity, where objects represent different stages of the manufacturing process (raw materials, preforms, unfinished beads, debris) along with the associated tools. Aside from a few exceptional discoveries (Rollefson 2002;

Byrd 2005; Thuesen and Kinzel 2018) or in some seasonal camps established within specific mineral landscapes exploitable for bead-making (Wright *et al.* 2008), identifying bead workshops in densely constructed prehistoric settlements is a challenging task. One should consider that:

- living in, or using structures was likely subject to cultural attitudes – such as cleaning, re-arranging, displacing, maintaining, *etc.* (Henry *et al.* 2014), which would harden the interpretation of the archaeological observations;
- “slow” techniques (abrasion, polishing, sawing, drilling) are those most applied for bead-making. Their debris consists of particles of abraded materials that are undetectable to the naked eye during excavation;
- the valuable character of the raw materials, which were generally procured from non-local sources, favours their protection and withdrawal after the required quantity had been extracted. In other words, remaining exploitable fragments would be kept away after their use, thus removed from the manufacturing context;
- working tools are also valuable and some, such as the drilling tools are additionally fragile. They would also be retrieved immediately after their use (Roux 2000).

Techno-Economic Investment

The technological characteristics of the stone and shell beads used for the necklace, reflect significant investments in time and energy during their manufacture. Over two thousand disc beads were integrated into the necklace's rows. Although their making benefited from batch polishing that accelerated the work considerably, in comparison to a single-bead treatment (Alarashi 2021), the previous shaping and perforation stages also require time and skills.

It is still unclear whether the disc beads were shaped and perforated one by one, or sliced from long tubular beads. It is worth reminding that the calcite tubular beads have a diameter range that corresponds to the range of the diameter of disc beads (within the main cluster observed in Fig. 21). It is thus likely that the tubular and disc calcite beads were linked to the same manufacturing process. Additionally, the necklace integrates seven flat beads made from the same reddish calcite. The transformation of this material into three different typological

families: the disc, the tubular, and the flat beads, within the same assemblage/ context has so far no parallel elsewhere at the site or in the Levant. At Ba`ja, tubular and flat beads made from striped fossil *Tridacna* occur together in some burials (DG1, CG9). “Jamila’s” necklace integrates only the tubular type. Based on these observations, the management of the raw materials and previously their accessibility, appear determinant in the diversification of types. The exploitation of the mother-of-pearl is subject to the same transformation strategies. Mainly oriented towards the production of large rings, the remaining mother-of-pearl fragments that are not suitable for standard types (*e.g.*, small rings, buttons) were transformed into a variety of objects – some being unique (Alarashi in this volume: Fig. 5). In sum, the principal components of the necklace (the mother-of-pearl ring, the stone and shell beads) were produced according to the same philosophy and know-how, namely, within the village of Ba`ja. In addition the beads were produced intelligently, thanks to optimisation strategies in the exploitation of the raw materials, and in the improvement of the work efficiency through batch processing of certain types. The high skills required, the standardisation and harmonisation of sizes, and the techno-economic strategies hint to well-organised bead crafting involving specialised artisan(s).

Between Cultural Choices and Regional Markers

The types of beads, the colours, and the materials used for the necklace are generally coherent with the ornamental spectra of the Late PPNB cultures (*e.g.*, Wright and Garrard 2003; Bar-Yosef Mayer 2005, 2013; Maier 2008; Al Nahar 2014; Alarashi 2014; Spatz *et al.* 2014; Thuesen and Kinzel 2018). Whereas disc (Bar-Yosef Mayer 2013; Baysal 2017) and (to a lesser extent) tubular beads are quite common since the beginning of the Neolithic in the Near East, flat beads with bi-convex sections are typical of the Late PPNB. In Northern Mesopotamia (Alarashi 2016) and Anatolia (Yelözer and Alarashi 2021) this type is found in a variety of geometric shapes and impressive sizes, using hard materials such as carnelian, agate, amazonite, turquoise, obsidian, and other semi-precious stones. Those found at Ba`ja are on the contrary rather small and made from soft materials such as the calcite specimens of the necklace, or others diamond-shaped made from *Tridacna* found

elsewhere at the site. The use of *Tridacna* for this type has been recorded at the contemporaneous site of Basta (Hermansen n.d.) but is otherwise rare in the Levant. At Ba`ja its use could have been inspired by the whitish colour offered by the material. For the child's necklace, the white colour was represented almost exclusively by the tubular shells and the mother-of-pearl ring (beside the four tiny *Conus* ring beads and an isolated *Dentalium* bead). It contrasted with the reddish calcite disc, tubular, and flat beads. The latter being quite small and not too distinguishable from the other tubular or disc beads – their use within the necklace may have had symbolic functions related to childhood. In Northern Mesopotamia and Anatolia the flat or “butterfly” beads are mainly found in burials of subadults (Alarashi 2016; Yelözer and Alarashi 2021).

The reason for the use of the four tiny *Conus* discs and one short section of *Dentalium* that were hardly visible among the densely beaded cords of the necklace, is difficult to discern from a visual or aesthetic point of view. The same holds true for the two amber beads. It is the first time, that fossil resin beads were determined for this early period. They are exceptional from an archaeological point of view. Whether their use for the child's necklace encodes symbolic functions, values, or prestige remains unclear, as further investigation is needed to explore their occurrence (Hermansen 2004), their manufacturing process (Moorey 1999) and their potential sources in prehistoric times in the region (Bandel *et al.* 1997; Nohra *et al.* 2013). Unlike the stone beads, the mother-of-pearl rings and their derivate types (such as the decorated flat type made for the necklace, and the tubular *Tridacna* beads) seem to occur only in Ba`ja and the neighbouring contemporaneous mega-site of Basta (Hermansen 2004). They appear as regional markers and are akin to define the ornamental tradition of the Greater Petra Area.

The mother-of-pearl ring played a key-role in the display of the necklace, through the organisation and the spread of the rows on the chest. While the canalisation of the rows from each side towards the back of the neck can simply be made by knots or stiches, two almost identical large spherical beads were possibly used for this purpose. Likewise, the rows could have been simply attached together behind the neck. Nonetheless, the artist used an elegant attractive black large buckle to receive the rows from each side. The couple of spherical beads and the

buckle were all made from dark grey hematite, a dense and resistant material. Together with the mother-of-pearl ring, which is the largest item of the necklace, they were essential for its display and symmetry, and above all, for its impressive aspect. Its design is highly sophisticated, and its creation was pursued down to the finest details.

Conclusion

The child's necklace represents a unique discovery never attested anywhere in the Levant for the 8th and 7th millenniums BCE. The combination of specific types, sizes, and colours of beads within a preconceived composition suggests high artistic standards rooted in the symbolic substratum of the local Late PPNB communities. Considering ornaments from other child burials at Ba`ja, it seems that two types – the flat (“butterfly”) beads and the mother-of-pearl rings – were most often associated with children and may have also been chosen intentionally for this necklace to indicate childhood (although it must be kept in mind that only very few children were decorated with such prestigious objects). On the other hand, comparing the combination of bead types and the colours of this ornament with others uncovered at Ba`ja, indicates that this composition was unique and very specific to this particular child. The selection of the composing elements – the turquoise beads may be an exception – was likely not a matter of availability but rather of choice, from a common repertoire.

Most likely the local production of the mother-of-pearl ring and possibly also of the *Tridacna* and calcite beads, demanded high artistic skills. Whether the other beads (hematite and turquoise) which show intensive use-wear traces were exchanged from other communities or handed over for generations, remains an open question. The differences in use-wear intensity of the rare exotic types and of the other, probably locally produced, beads are striking, and open the door for further speculations. Was the necklace assembled especially for the burial ritual of the child? Had the ornament elements been assembled and threated anew several times until they were finally ex-commodified? Considering the strong use-wear of the hematite beads and of the buckle, leads us to assume that the latter objects were used intensively, possibly for many years. Such a necklace attributed a special status to the person who wore it, but also to the persons who ex-commodified it. It was

not a daily-life ornament but rather an extremely prestigious item used for special occasions (death being one of them). Nonetheless, it was withdrawn from the life cycle to accomplish other symbolic functions.

Irrespective of the location of the bead production, the exotic raw materials used indicate participation and possibly entanglements in supra-regional networks (Red Sea, Sinai, southeastern steppe). The ex- or de-commodification of such a valuable object in a burial ritual, is all the more remarkable. Its association with a child reaffirms the significant place of children within Neolithic communities, and even their indirect role in stimulating techno-economic, artistic and cultural systems. Indeed, the study of the necklace reveals how complex the

interactions between the involved social actors of the community of Ba`ja may have been – the bead-makers, the string/ cordage makers, the travellers, or mobile individuals, the familial or tribal authorities behind the demands or artistic creations, and other members of the society – all able to decode the significance of the necklace and to interact through criticism, aspiration, or rejection. The necklace reflects a complex narrative of the social dynamics in and outside Ba`ja that certainly merit further exploration.

Hala Alarashi

Spanish National Research Council
(IMF-CSIC), Barcelona
alarashi.hala@gmail.com

References

- Abu Laban A.
2014 The use of marine shells at the Neolithic site Shkarat Msaied, Jordan. In: K. Szabó, C. Dupont, V. Dimitrijević, L. Gómez Gastélum and N. Serrand (eds.), *Archaeomalacology: shells in the archaeological record*. British Archaeological Reports, international series 2666: 9-17. Oxford: Archaeopress.
- Al Nahar M.
2014 ‘Ain Ghazal and Wadi Shueib: Neolithic personal ornaments. In: B. Finlayson and C. Makarewicz (eds.), *Settlement, survey, and stone: essays on Near Eastern Prehistory in honor of Gary Rollefson*: 243-256. Berlin: ex oriente.
- Alarashi H.
2014 *La parure épipaléolithique et néolithique de la Syrie (12e au 7e millénaire avant J.-C.) : techniques et usages, échanges et identités*. PhD. Thesis. Lyon: Université Lumière-Lyon 2.
2016 Butterfly beads in the Neolithic Near East: evolution, technology and socio-cultural implications. *Cambridge Archaeological Journal* 26: 493-512. doi:10.1017/S0959774316000342
2021 New insights into the technological management of the Neolithic cowrie beads in the Levant. An experimental and traceological approach. In: S. Beyries, C. Hamon and Y. Maigrot (eds.), *Beyond use-wear traces: going from tools to people by means of archaeological wear and residue analyses*: 173-186. Leiden: Sidestone.
- Alarashi H., Ortiz A. and Molist M.
2018 Sea shells on the riverside: cowrie ornaments from the PPNB site of Tell Halula (Euphrates, northern Syria). *Quaternary International* 490: 98-112. doi:10.1016/j.quaint.2018.05.004
- Bandel K., Shinaq R. and Weitschat W.
1997 First insect inclusions from the amber of Jordan (Mid Cretaceous). *Mitteilungen aus dem Geologisch-Paläontologischen Institut der Universität Hamburg* 80: 213-223.
- Bar-Yosef Mayer D.E.
2005 The exploitation of shells as beads in the Palaeolithic and Neolithic of the Levant. *Paléorient* 31: 176-185. doi:10.3406/paleo.2005.4796
2013 Towards a typology of stone beads in the Neolithic Levant. *Journal of Field Archaeology* 38: 129-142. doi:10.1179/0093469013Z.000000000043
- Baysal E.
2017 Personal ornaments in Neolithic Turkey, the current state of research and interpretation. *Journal of Archaeology and Art* 155: 1-22.

- Benz M., Alarashi H., Gresky J., Purschwitz C. and Gebel H.G.K.
2023 Moments of memory and belonging. A special child burial from Neolithic Ba`ja, southern Jordan. In: E. Murphy and M. Le Roy (eds.), *Normative, atypical or deviant? Interpreting Prehistoric and Protohistoric child burial practices*: 10-31. Oxford: Archaeopress.
- Benz M., Gresky J. and Alarashi H.
2020 Similar but different: displaying social roles of subadults in burials from the late Pre-Pottery Neolithic site of Ba`ja, southern Jordan. In: H. Alarashi and R.M. Dessi (eds.), *L'art du paraître apparences de l'humain, de la Préhistoire à nos jours. Actes des rencontres, 22-24 Octobre 2019, Nice*: 93-107. Nice: Editions APDCA - CEPAM.
- Benz M., Gresky J., Štefanisko D., Alarashi H., Knipper C., Purschwitz C., Bauer J. and Gebel H.G.K.
2019 Burying power: new insights into incipient leadership in the late Pre-Pottery Neolithic from an outstanding burial at Ba`ja, southern Jordan. *PLoS One* 14: e0221171. doi:10.1371/journal.pone.0221171
- Byrd B.F.
2005 *Early village life at Beidha, Jordan: Neolithic spatial organization and vernacular architecture*. British Academy Monographs in Archaeology 14. Oxford: Oxford University Press.
- Critchley P.
2007 The stone beads. In: B. Finlayson and S.J. Mithen (eds.), *The early Prehistory of Wadi Faynan, Southern Jordan: archaeological survey of Wadis Faynan, Ghuwayr and al-Bustan and evaluation of the Pre-Pottery Neolithic A site of WF16*. Levant supplementary series: 356-361. Oxford: Oxbow.
- Francis P.J.
1989 The manufacture of beads from shell. In: C.F. Hayes (ed.), *Proceedings of the 1986 shell bead conference*. Research Records 20: 25-35. Rochester: Rochester Museum and Science Center.
- Gebel H.G.
1988 Late Epipalaeolithic and aceramic Neolithic sites in the Petra Area. In: A.N. Garrard and H.G. Gebel (eds.), *The Prehistory of Jordan. The state of research in 1986*: 67-100. Oxford: BAR.
- Gebel H.G.K. and Hermansen B.D.
2001 LPPNB Ba`ja 2001. A short note. *Neo-Lithics* 2/01: 15-20.
- Gebel H.G.K., Benz M., Purschwitz C., Alarashi H., Bauer J., Gresky J., Heidkamp B., Abuhelaleh B., Miškolciová L., Keßeler A., Kubíková B., Štefanisko D., Strauss M. and Wellbrock K.
2019 Household and death, 2: preliminary results of the 12th season (2018) at late PPNB Ba`ja, southern Jordan. *Neo-Lithics* 19: 20-45.
- Gebel H.G.K., Benz M., Purschwitz C., Bader M., Dermech S., Graf J., Gresky J., Hájek F., Miškolciová L., al-Khasawneh S., Khrisat B., Kubíková B., Renger M., Wellbrock K., al-Sababha H.M. and al-Shoubaki S.
2020 Household and death, 3: preliminary results of the 13th season (spring 2019) at Late PPNB Ba`ja, southern Jordan. *Neo-Lithics 20 Special issue, Ba`ja 2019 season, interim report*: 3-41.
- Gebel H.G.K., Benz M., Purschwitz C., Kubíková B., Štefanisko D., Al-Souliman A., Tucker K., Gresky J. and Abuhelaleh B.
2017 Household and death: preliminary results of the 11th season (2016) at late PPNB Ba`ja, southern Jordan. *Neo-Lithics* 1/17: 18-36.
- Groman-Yaroslavski I., Rosenberg D. and Nadel D. (eds.)
2013 *Stone tools in transition: from hunter-gatherers to farming societies in the Near East: papers presented to the 7th conference on PPN chipped and ground stone industries of the Fertile Crescent*. Barcelona: Universitat Autònoma de Barcelona.
- Hauptmann A.
2004 "Greenstones" from Basta. Their mineralogical composition and possible provenance. In: H.J. Nissen, M. Muheisen and H.G.K. Gebel (eds.), *Basta 1: the human ecology*. bibliotheca neolithica Asiae meridionalis et occidentalis and Monograph of the Faculty of Archaeology and Anthropology 4: 169-176. Berlin: ex oriente.
- Henry D.O., Kadowaki S. and Bergin S.M.
2014 Reconstructing early Neolithic social and economic organization through spatial analysis at Ayn Abu Nukhayla, southern Jordan. *American Antiquity* 79: 401-424.
- Hermansen B.D.
2004 Raw materials of the small finds industries. In: H.J. Nissen, M. Muheisen and H.G.K. Gebel (eds.), *Basta 1: the human ecology*. bibliotheca neolithica Asiae meridionalis et occidentalis

- and Monograph of the Faculty of Archaeology and Anthropology 4: 117-125. Berlin: ex oriente.
- n.d. The small finds and ornaments industries. In: B.D. Hermansen, H.G.K. Gebel and D. Reese with a contribution by K. McNamara (eds.), *Basta 4.1: The small finds and ornament industries*. bibliotheca neolithica Asiae meridionalis et occidentalis. Berlin: ex oriente.
- Kaur S., Stout E., Kaur T. and Estridg V.
2012 Infrared spectroscopy of amber samples from the Artemision excavations of 1904/1905. *Anatolia Antiqua* 20: 39-43. doi:10.3406/anata.2012.1325
- Maier R.
2008 "Grünsteine" und "Grünstein"-Perlen aus Beidha. Jordanien. M.A. Thesis n.d. Bochum: Ruhr University.
- Maréchal C. and Alarashi H.
2008 Les éléments de parure de Mureybet. In: J.J. Ibáñez (ed.), *Le site néolithique de Tell Mureybet (Syrie du Nord)*. British Archaeological Reports, international series 1843 (II): 575-617. Oxford, Lyon: BAR, Maison de l'Orient et de la Méditerranée.
- Moorey P.R.S.
1999 *Ancient Mesopotamian materials and industries: the archaeological evidence*. Winona Lake: Eisenbrauns.
- Nohra Y., Azar D., Gèze R., Maksoud S., El-Samrani A. and Perrichot V.
2013 New Jurassic amber outcrops from Lebanon. *Terrestrial Arthropod Reviews* 6: 27-51. doi:10.1163/18749836-06021056
- Purschwitz C.
2017 *Die lithische Ökonomie von Feuerstein im Frühneolithikum der Größeren Petra Region*. Studies in Early Near Eastern Production, Subsistence, and Environment 19. Berlin: ex oriente.
- Rollefson G.O.
2002 Bead-making tools from LPPNB al-Basit, Jordan. *Neo-Lithics* 2/02: 5-7.
- Roux V.
2000 *Cornaline de l'Inde: des pratiques techniques de Cambay aux techno-systèmes de l'Indus*. Paris: Editions de la Maison des Sciences de l'Homme.
- Spatz A.J., Bar-Yosef Mayer D., Nowell A. and Henry D.O.
2014 Ornaments of shell and stone: social and economic insight. In: D.O. Henry and J.E. Beaver (eds.), *The sands of time. The desert Neolithic settlement at Ayn Abū Nukhayla*. bibliotheca neolithica Asiae meridionalis et occidentalis: 245-258. Berlin: ex oriente.
- Thuesen M.B. and Kinzel M.
2018 Stone beads from Shkārāt Msaied. *Neo-Lithics* 1/18: 3-7.
- Wright K. and Garrard A.
2003 Social identities and the expansion of stone bead-making in the Neolithic Western Asia: new evidence from Jordan. *Antiquity* 77: 267-284.
- Wright K.I., Critchley P., Garrard A., Baird D., Bains R. and Groom S.
2008 Stone bead technologies and early craft specialization: insights from two Neolithic sites in Eastern Jordan. *Levant* 40: 131-165. doi:10.1179/175638008X348016
- Yelözer S. and Alarashi H.
2021 "Yaşamda ve Ölümde" - Akeramik Neolitik Dönem'de Boncuklar ve Kimlikler, Aşıklı Höyük Örneği, "In Life and in Death" – beads and identities during the aceramic Neolithic period, the case study of Aşıklı Höyük. In: A. Günal Türkmenoğlu and Ş. Demirci (eds.), *Türkiye Arkeolojisinde Takı ve Boncuk: Arkeolojik ve Arkeometrik Çalışmalar*: 81-93. Istanbul: Ege Yayınları.